Aus der Medizinischen Klinik und Poliklinik II
Klinik der Ludwig-Maximilians-Universität München
Direktorin Prof. Dr. med. Julia Mayerle

Potential new biomarkers for liver diseases——
SEPT6 and serum zinc levels

Dissertation
zum Erwerb des Doktorgrades der Humanbiologie
an der Medizinischen Fakultät
der Ludwig-Maximilians-Universität zu München
vorgelegt von
Yuhui Fan
Aus
Shanxi
2021

Mit Genehmigung der Medizinischen Fakultät
der Universität München

Berichterstatter: Prof. Dr. med. Christian Steib

Mitberichterstatter: PD Dr. Stefan Gölder
Prof. Dr. Norbert Grüner

Dekan: Prof. Dr. med. Thomas Gudermann

Tag der mündlichen Prüfung: 26.10.2021

LMU LUDWIG-MAXIMILIANS-UNIVERSITÄT MÜNCHEN

Dean's Office
Faculty of Medicine

MMRS

Affidavit

Fan, Yuhui

Surname, first name

Street

Zip code, town

Country

I hereby declare, that the submitted thesis entitled

Potential new biomarkers for liver diseases—— SEPT6 and serum zinc levels

is my own work. I have only used the sources indicated and have not made unauthorised use of services of a third party. Where the work of others has been quoted or reproduced, the source is always given.

I further declare that the submitted thesis or parts thereof have not been presented as part of an examination degree to any other university.

Munich, 27. 10. 2021

Place, date

Yuhui Fan

Signature doctoral candidate

Table of Contents

1 Abbreviations

SEPT6	Septin 6
HCC	Hepatocellular carcinoma
qRT-PCR	Quantitative real-time PCR
WB	Western blot
IHC	Immunohistochemistry
PVDF	Polyvinylidene difluoride
BSA	Bovine serum albumin
CCK-8	Cell Counting Kit-8
PI	Propidiumiodide
GEPIA	Gene Expression Profiling Interactive Analysis
MMP	Matrix metalloproteinase
CCND1	Cyclin D1
LATS1	Large Tumor Suppressor Kinase 1
YAP	Yes-associated protein
TEAD	TEA domain family member
CLD	Chronic liver disease
HSC	Hepatic stellate cells
KC	Kupffer cell
CRP	C-reactive protein
TMC	THP-1 macrophage
PAMP	Pathogen-associated molecular pattern
PMA	Phorbol myristate acetate
SBP	Spontaneous bacterial peritonitis
SEC	Sinusoidal endothelial cells
E.coli	Escherichia coli
E. Cloacae	Enterobacter cloacae
E. Faecium	Enterococcus faecium
S. Pneumoniae	Streptococcus pneumoniae
LDH	Lactate dehydrogenase
Myd88	Myeloid differentiation factor 88
MAPK	Mitogen-associated protein kinase
NF-κB	Nuclear factor-kappa B
IRAK-1	Interleukin receptor- associated kinase-1

2 Publication list

2.1 Publication 1

SEPT6 drives hepatocellular carcinoma cell proliferation, migration and invasion via the Hippo/YAP signaling pathway. Int J Oncol. 2021 Jun;58(6):25.
doi: 10.3892/ijo.2021.5205. Epub 2021 Apr 13.

Yuhui Fan, Zhipeng Du, Qiang Ding, Jiang Zhang, Mark op den Winkel, Alexander L. Gerbes, Mei Liu, Christian J. Steib

2.2 Publication 2

Pretreatment with Zinc protects Kupffer cells following administration of microbial products. Biomed Pharmacother. 2020 Jul;127:110208.
doi: 10.1016/j.biopha.2020.110208. Epub 2020 May 14.

Jiang Zhang, Andreas Wieser, Hao Lin, **Yuhui Fan**, Hanwei Li, Tobias S. Schiergens, Julia Mayerle, Alexander L. Gerbes, Christian J. Steib

3 Contribution to the Publications

3.1 Contribution to paper I

Yuhui Fan is the first author of the paper I, she performed most of the cytologic and mechanistic experiments, analyzed the experimental data, and revised the manuscript.

3.2 Contribution to paper II

Yuhui Fan shared the co-authorship as the fourth author in paper II, she made substantial contributions to the conception of the study and helped to draft the manuscript.

4 Introduction

4.1 An overview of HCC

The heterogeneous disease Hepatocellular carcinoma (HCC) has shown an increasing incidence and fatality rate, it is a widely common malignance and the third primary cause of the cancer-related deaths across the globe [1]. And just recently, the HCC incidence rate approached its fatality rate which is due to the direct relationship between chronic inflammation, chronic viral infection, hepatocellular carcinoma and hepatotoxins. Around one million patients die every year due to this disease around the world. additionally, less than half of the patients (40%) are diagnosed in its early stages [2], where they reach the point where surgeries are no longer viable, while both the chemotherapy and the radiotherapy do not exhibit potency against HCC [3] .The poor prognosis with overall survival rates of 3-5% is mainly due to the distant metastasis, so it must be significant to pinpoint the foreboding HCC biomarkers. There has been a significant advancement in identifying and curing HCC over the past few years. With the systemic therapies being the foundation of the advanced stage patients treatment.

4.2 Septin family

Septin family, a gene family with GTPase activity in all eukaryotes except plants[4]. Mostowy et al. found that the protein members encoded by the genes of this family are huge.As a scaffold for protein interactions, septins participate in a series of important biological behaviors and physiological processes such as the regulation of cell cycle progression, apoptosis, and cell polarization. More and more evidence shows that the septin family is closely related to the development of some malignant tumors and neurodegenerative diseases like leukemia, Parkinson's disease, Alzheimer's disease, prostate and colorectal cancers.

The microfilaments formed by the septin protein complex serve as scaffolds to recruit and activate other proteins. Through their scaffolding, they also become important constituents of membrane-associated proteins. The complex signaling pathways of various gene proteins between the septin family make more and more people believe that septins may become a new target in anti-cancer treatment strategies [5]. Therefore, it is of great significance to focus on the relationship between the molecular and cellular pathophysiological mechanisms of septins' influence in cancer or other diseases.

4.3 Septin structure

A total of 13 human septin proteins have been discovered so far, and they could be split to 4 classes based on the affinity of their genetic structure [6]. The protein encoded by the septin gene family has a molecular mass of approximately 39 to 60 kDa [7]. Septins can be oligomerized into repetitive and ordered octamers or

hexamers that could form more developed structures, including loops or microfilaments. Septins are rod-shaped and filament-like, which is related to membranes, actin or microtubules (MTs), so it is therefore regarded to be the fourth component of the cytoskeleton [8]. According to the degree of sequence similarity, SEPT gene family members are divided into four different subfamilies. They are SEPT 2 subfamily (SEPT 1, 2, 4, 5), SEPT 3 subfamily (SEPT 3, 9, 12), SEPT 6 subfamily (SEPT 6, 8, 10, 11, 14) and SEPT 7 subfamily Family (SEPT 7, 13) [9].

4.4 Septin and biology behavior

4.4.1 Septin and mitosis

Through the formation of highly ordered loops at cell division sites, we found that septins play a significant part in the time-structure yeast germination control [9]. In mammalian cells, the septins are also considered to be one of the factors that contribute to mitosis. In fact, after the mediated Cdk1 phosphorylation, the long SEPT9 subtype becomes a medium for prolyl isomerase Pin1, and in order to achieve the cytokinesis its isomerization is a must [10]. similar to the Pin1 controlled other tumor suppressors and oncogenes, specific SEPT9 subtypes may be involved in tumorigenesis. In addition, Spiliotis et al. found that septins help to achieve correct chromosome expression and separation in the later stage. Thus, the SEPT2/6/7 complex is deemed crucial for the CENP-E recruitment, a protein that belongs to the family of kinesin involved in the end stage of mitosis [10].

At the end of mitosis, septins are concentrated in the central spindle area, and interacts with the actin contractile ring through the partnering protein aniline. Current data showed that the anillin-septin loop prompts the invasion, narrowing and elongation of intercellular bridges [11]. Recent research reported on the chrysotile asbestos fibers consequences (causing mesothelioma, asbestos and lung cancer) have highlighted that due to over-expression of SEPT2 and the occurrence of formaldehyde and SEPT9 dislocation, this is very common in cancer cells [12].

4.4.2 Septin and membrane structure

Through diffusion in the plasma membrane, septins self-assemble into a microtubule microfilament structure[13]. Therefore, large-scale septin microfilament arrays that interact stably with the plasma membrane can change the occurrence of cortical morphology by applying membrane curvature and affecting migrating cells' hardness, thereby contributing to tumor metastasis [14].

In addition, septins are also involved in growth factor receptors associated with cancer development dysregulation. They could aggregate and balance the proteins of the plasma membrane, including receptor tyrosine kinases[15]. In fact, the membrane-associated SEPT9 can prevent the binding of CIN85 to the ubiquitin ligase Cbl, leading to a reduction in ubiquitin-dependent degradation of EGFR [16]. In

addition, septins can persist on the cancer cells plasma membranes by reducing ubiquitination and degrading ErbB2. Furthermore, the c-Met proto-oncogene surface distribution is monitored by SEPT2 and 11 in the opposite manner, while both engage in its interplay with ligands and anchor to the cytoskeleton of actin, elucidating the subunits composed of septin microfilament can control the importance of biological functions [17].

4.4.3 Septin and actin

The structure of septin microfilament binds to the cortical area of actin in many cells. The loss of actin causes septin to form free cytoplasmic loops [18]. In contrast, the loss of SEPT2 weakens actin binding and destroys stress fibers. Knocking out SEPT6 and SEPT7 can produce similar actin bundle loss and destruction of polarity of the cells [19]. These ramifications can include septin binding partners that cross-link septin to actin, such as two of BORG2 and B5 of the five Cdc42 effectors in the BORG family [20].

The septin protein controls the remodeling of actin during cell migration and may therefore lead to the spread and invasion of metastatic cancer cells [21]. Septins help to stabilize neonatal focal adhesions, which is one of the necessary steps for tumor-related migration. The study found that the embryonic fibroblasts of SEPT9 knockout mice did migrate much slower than wild-type cells [22]. In addition, SEPT9_i4 is also associated in the directionality of breast cancer cell MCF7 migration. Further sustained directional migration depends on SEPT7 and BORG5, because it can maintain proper actin filament organization [23]. Cell invasion and migration require epithelial-mesenchymal transition (EMT), which encompasses cell processes formation and alters the way cells interact with ECM. Studies have found that knocking out SEPT9 can reverse EMT and reduce the spread, migration and invasion of cancer cells [24]. In addition, SEPT1 is also associated with the spreading of DJM-1 cells in the squamous cell carcinoma[24].

Septins are involved in tumor progression, including the formation of new blood vessels and the transition of tumor cells into the tumor microenvironment. ECM controls the expression of SEPT9 in endothelial cells through integrin signaling and regulates the peripheral distribution of cell proliferation and actin assembly [25]. Concerning the migration of tumor-related fibroblasts, studies have shown that due to the increased expression of the cross-linked protein BORG2, the cohesion between septins and actin fibers increases [26]. This will lead to matrix remodeling, which will help activate highly contracted cancer-related fibroblasts and promote the invasion of cancer cell, angiogenesis, and tumor growth.

4.4.4 Septin and microtubules

In some types of cells, septin filaments are co-paired with MTs. They compete with the MT-stable protein MAP4 and reduce MT stability [27]. However, the relation between septins and MT acetylation remains ambiguous. In dendritic cells, SEPT7 is recorded interacting with tubulin deacetylase HDAC6 [28]. Additionally, septin microfilaments interact with polyglutamylated MTs and facilitate the transport of vesicles along these trajectories to sustain the polarity of MDCK cells [29].

Septins don't only form a barrier to diffuse at the base of primary cilia, but also associated with acetylated MTs in the axons of RPE-1 cells whose SEPT2/7/9 complex controls ciliary body length [30]. Loss of TTLL3 activity, a polysaccharide acylation enzyme needed for a stable primary cilia genesis is closely related to the development of colon cancer [31]. Similar to the study of septin microfilaments recruiting tubulin polyglutaminase on MTs, axon-related septin may scaffold TTLL3 on cilia MTs because it is a part of the same enzyme family [32].

4.5 Septin with disease

4.5.1 Hereditary neuromuscular dystrophy (HNA)

HNA is a rare autosomal dominant inherited peripheral neuropathy characterized by severe pain and weakness in the shoulders and/or arms, loss of feeling and atrophy of the arm muscles. The patient usually recovers completely, but it may take weeks to years. Genetic analysis of several HNA patients and their families identified mutations in the SEPT9 gene [33]. To date, missense mutant subtypes R88W or S93F have been found in some HNA families (the longest numbered SEPT9 subtype) [34]. In addition, a repeat containing the SEPT9 gene was also detected, in which the length and position of the repeated part SEPT9 were different. Interestingly, point mutations and gene duplication occur in the N-terminal region shared by isomers 1, 2 and 3 of SEPT9, but not 4 and 5, indicating the importance of this region for the onset of HNA [35].

4.5.2 Male infertility

A group of patients infertile due to decreased sperm motility (azoospermia) showed disintegration of ring and septin rings. Septins provide rigidity at the ring and acts as a diffusion barrier to distinguish different parts of sperm. Specifically, SEPT4-deficient mice can lead to loss of sperm motility, and studies have found that SEPT4 is essential for the barrier between the midsection and the tail [36]. Although the loss of SEPT4 has been detected in infertile human males, the cause of SEPT4 loss remains to be determined. The importance of SEPT4 and whether it provides cell rigidity or diffusion barrier function needs further verification.

4.5.3 Leukemia (MLL)

Septins are associated with various human MLL caused by the translocation of the MLL oncogene to the septin gene locus [37]. MLL is located on chromosome 11q23, a locus frequently involved in chromosomal translocations associated with leukemia [38]. Although more than 60 different MLL gene translocations have been identified so far, 5 of them involve members of the septin family, making it unlikely that this will happen by accident. These translocations have caused a variety of acute leukemias. The first described septin was fused to the MLL gene located on chromosome 11, resulting in the chimeric protein containing the N-terminal region of MLL linked to SEPT9 [39].

Other septins (SEPT2, SEPT5, SEPT6, and SEPT11) were later reported to have experienced similar translocations and produced fusion proteins with MLL [40]. This fusion protein is thought to lead to leukemia progression through excessive activation of MLL, leading to unnecessary transcription of certain genes including members of the HOX family [41, 42]. Septin's contribution to this activation is unclear, but may involve their self-interacting properties that may lead to MLL dimerization [43]. In addition, their association with membranes or other components of the cytoskeleton can also play a role. Osaka et al. identified septins as the fusion partner for leukemia MLL and found that in many cancer cells, SEPT2, 8, 9, and 11 are up-regulated, while SEPT4 and 10 are down-regulated [44, 45].

4.5.4 Breast and ovarian cancer

The study found that the SEPT9 gene is closely related to breast and ovarian cancer. The human SEPT9 locus has been identified as a hot allele in ovarian and breast cancer. SEPT9 gene amplification can also be found in human and mouse breast cancer cell lines [46].

4.5.5 Head and squamous sell carcinoma

Studies have found that strong expression of Sept9_i1 is linked to head and squamous cell carcinoma poor prognosis. The frequency of methylation at the SEPT9 site indicates that changes in the SEPT9 subtype may result in a malignant phenotype [47].

4.5.6 Colorectal cancer (CRC)

The experiment found that SEPT9 is closely related to colorectal cancer. The decrease in expression may be due to the reduction in the transcription frequency of the promoter and its methylation of CpG islands [48]. Consistent with this, treatment of cultured cells with demethylating agents resulted in increased levels of SEPT9 mRNA and protein. This methylation change has recently been used to diagnose the colon

cancer using blood-based SEPT9 gene promoter methylation detection [49]. Because it is minimally invasive, it may have a higher participation rate than colonoscopy [50, 51]. These findings not only point out a new treatment method, but also provide a new, effective and non-invasive diagnostic method for the diagnosis of colorectal cancer.

4.6 Aim of the study

4.6.1 SEPT6 drives proliferation, migration and invasion of hepatocellular carcinoma through Hippo/YAP signaling pathway（Publication 1）

The gathered data proposes that the cytoskeleton proteins are essential for the hepatocellular carcinoma tumorigenesis. Yet, the exact SEPT6 function in the hepatocellular carcinoma is still unrevealed. In this study, by utilizing RT-PCR and the western blot assay, we were able to identify the expression of SEPT6 in HCC cell lines, as well as identifying the role of SEPT6 in proliferation, cell cycle progression, invasion and migration of HCC by carrying out a gain- and loss- of function assays. Furthermore, we examined the underlying mechanism focused on the Hippo signaling, since that this pathway is crucial in progression and tumorigenesis of HCC. Our findings demonstrated that the Hippo signaling is inhibited by the overexpression of SEPT6, and that SEPT6 also affected the downstream effector YAP by stabilizing and dephosphorylating it, and as a consequence, the active YAP is translocated to the nucleus, so it could boost the Cyclin D1 and MMP2 transcription, leading to the metastasis and growth of HCC. These gathered data as a whole have the potential to yield a therapeutic intuition in the treatment of HCC. The data is published in Publication1

4.6.2 Pretreatment with Zinc protects Kupffer cells following administration of microbial products（Publication 2）

The severe liver fibrosis and the systemic inflammation can prompt a decline in the concentration of the serum zinc. Nonetheless, the absence of any symptoms for zinc deficiency leads it to be undetected in clinics. This research explored the relationship between the serum zinc and the other indicators in CLD patients, in correlation with the zinc protective mechanisms in SBP infections. And we found that: 1) there is a direct correlation between deficient serum zinc concentrations and elevated MELD scores and CRP levels in CLD patients , where 60 μg/dl is established to be the zinc deficiency threshold; 2) There is a major LDH surge in both HSCs as well as KCs induced by the bacterial products, yet, Only KCs but not HSCs, are preserved by the zinc pretreatment; 3) Zinc pretreatment exhibited guarding features in KCs rather than zinc posttreatment and these features are propagated through Myd88-MAPK-related pathway; 4) The pretreatment of zinc decreases the TXB2 production in KCs otherwise caused by bacterial stimulation. In a word, the levels of serum zinc seem to be an important indicator in evaluating the severity of the CLD patients with infection and liver fibrosis. The data were published in Publication 2.

5 Summary

Publication 1:

SEPT6 drives proliferation, migration and invasion of hepatocellular carcinoma through Hippo/YAP signaling pathway

The gathered data proposes that the cytoskeleton proteins are essential for the hepatocellular carcinoma tumorigenesis. Septin 6 (SEPT6) is considered to be a highly evolutionarily conserved GTP binding protein, which takes a crucial part in regulating the biological behaviors of various cells, like actin dynamics, cell migration and shape and more, Yet, the exact SEPT6 function in the Hippo signaling and the hepatocellular carcinoma is still unrevealed. In this research, we revealed the function of SEPT6 in hepatocellular carcinoma and the underlying mechanism.Thereby, our study focused on the research of SEPT6 in hepatocellular carcinoma and the underlying mechanism was discovered in this research.

In order to inspect the SEPT6 function in HCC we determined the SEPT6 expression in 64 HCC sample pairs using qRT-PCR. Meanwhile,the expression of SEPT6 in both HCC as well as the adjacent non-tumor tissues was traced by the western blot. he correlation of SEPT6 expression with overall survival using Kaplan-Meier survival analysis was then studied, which showed that the elevated SEPT6 expression level is correlated with a poorer survival rate for HCC patients.Moreover, the SEPT6 expression in the database of GEPIA further confirmed the SEPT6 mRNA level upregulation in the tissues of HCC. Subsequently,we utilized IHC staining in order to examine the SEPT6 expression in the samples of HCC and non-tumor samples, we discovered that the levels of SEPT6 expression were noticeably higher in the HCC samples when compared to the non-tumor adjacent samples, while the expression of SEPT6 protein was predominantly situated in the cytoplasm. Lastly, we assessed the SEPT6 expression in the normal hepatocytes (Chang liver) as well as 5 HCC cell lines. Both the WB and qRT-PCR results demonstrated that the expression of SEPT6 was remarkably elevated in those characterized by large metastatic potential HCC cell lines (MHCC-97H and HCC-LM3) when compared to the regular hepatocytes (Chang liver). All these data pointed out that the expression of SEPT6 is upregulated in human HCC and that it predicts bad prognosis

We also carried out a loss- and gain- of function assays in order to inspect the role of SEPT6 in HCC proliferation and other cellular functions. The qRT-PCR and western blot both confirmed the successful stable knockdown efficiency of SEPT6 in the cells of MHCC-97H as well as the overexpression efficiency in Huh7 cells. We then carried out the CCK-8 assays in order to assess the function of SEPT6 in the proliferation of cells. We observed the cell cycle distribution via FACS in order to check if the proliferation is regulated by SEPT6 via altering the cell cycle transition. The findings proposed that SEPT6 advanced the transition of G1/S cell cycle in HCC cells.

Consequently, we recognized the cyclin D1 and cyclinE1 expression, that is substantially linked to transition of G1/S cell cycle. Afterwards, we carried out Transwell assays and were able to recognize the MMP2 and MMP9 expression via qRT-PCR and WB to examine both the HCC cells invasion and migration capabilities after both the overexpression and the knockdown. Lastly, we discovered that the overexpression of SEPT6 in vitro significantly prompted the HCC proliferation, cell cycle migration, invasion, and progression, while the SEPT6 suppression imposed the counter effects on HCC cell lines. Hence, we recognized SEPT6 as an oncogene in HCC, contrasting to its function in the prostate cancer.

Afterwards, the underlying mechanism why SEPT6 acts as an oncogene was explored. The Hippo signaling as the pathway plays vital role in HCC tumorigenesis and progression was mainly studied. T Our findings demonstrated that the overexpression of SEPT6 inhibited the Hippo signaling pathway as well as stabilizing and dephosphorylating the downstream effector YAP, as a consequence, the active YAP, boosted the Cyclin D1 and MMP2 transcription when it is translocated to the nucleus, leading to the metastasis and growth of HCC. Moreover, the YAP knockdown reduced the function of SEPT6 in the progression of HCC, whilst the overexpression of YAP preserved the suppressing function of SEPT6 downregulation. Accordingly, SEPT6 applied its oncogenic abilities in HCC by regulating the Hippo/YAP signaling pathway.

To conclude, our research proposed that SEPT6 is upregulated in HCC and that it acts as oncogene in the progression of HCC. We also documented that SEPT6 is prompting the HCC proliferation, cell cycle migration, invasion and progression, where is at least via an innovative SEPT6/Hippo/YAP axis. All in all, our data displayed that SEPT6 plays an oncogenic role in HCC, that can administer a therapeutic target in the treatment of HCC.

Publication 2:

Pretreatment with Zinc protects Kupffer cells following administration of microbial products

Zinc is a crucial trace metal to maintain human functions, and it is vital in about 300 enzymes for their formation and functionality. Moreover, zinc exhibits antioxidizing and antiapoptotic abilities, and it is widely used in anti-bacterial pathogens studies. The serum zinc levels can be severely hindered by systemic inflammation and severe fibrosis, on the other hand, the supplementation of patients by zinc is shown to enhance their Chronic liver disease (CLD) prognosis. Even though that the zinc associated medications proved its vitality, there has been no universal agreement on the dosage, timing and the mechanism of the effects yet. Bacterial isolates collected from SBP patients isolated strains are used to treat the human primary liver non-parenchymal cells such as HSCs, KCs and sinusoidal endothelial cells (SECs) in

this research, and the clinical data gathered throughout 2016 to 2019 was aggregated, in order to inspect the role of zinc in suppressing the microbial infections as well as the clinical application of zinc for CLD patients.

According to serum zinc levels, 149 CLD patients were split to three groups. The markers related to infection and fibrosis were compared. The findings showed a major inverse correlation between serum zinc levels and CRP and a major direct correlation between serum zinc and albumin in the both groups.

In in-vitro experiments, the human liver non parenchymal cells were triggered by microbial isolates extracted from patients, and in certain cases the solution of zinc sulfate was added. By comparing the effect of zinc by LDH and thromboxane A2 (TXA2) levels in the cell supernatant, the study intended to explore the clinical effects of the serum zinc in CLD patients as well as its protective effects in in-vitro experiments. We found that zinc pretreatment could protect the injury of bacterial stimulation in TMCs. Patients with deficient serum zinc levels showed more C-reactive protein (CRP), GGT, INR, total bilirubin, MELD score as well as lower albumin levels compared to other groups. There is a prevalent correlation between serum zinc with CRP and Albumin in both the groups with low and normal zinc levels, LDH levels were surged in Kupffer cells (KCs) as well as stellate cells by bacterial isolates, However, it did not show any impact on the sinusoidal endothelial cells, where the pretreatment by zinc only protected the KCs.

Finally, we investigated the potential associated pathway for zinc protection by RT-qPCR, and found that Myd88 related signaling pathway was vital for the protecting zinc pretreatment impacts in bacterial-induced injury in KCs, and reduced production of thromboxane A2 was due to decreased gene expression of Myd88, MAPK and NF-kB.

In summary, the levels of serum zinc show a high probability of being a worthy weapon in evaluating the mass of the infection and liver fibrosis in CLD patients. Moreover, the findings reinforced our comprehension of the supplementation by zinc as a viable antimicrobial ally where the pretreatment by zinc is shown to constrain inflammation through suppressing Myd88-MAPK-NF-κB pathway activation in KCs, and TXA2 as an important player.

6 Zusammenfassung

Veröffentlichung 1:

SEPT6 fördert die Tumorprogression über den Hippo/YAP-Signalweg beim hepatozellulären Karzinom

Akkumulative Studien haben gezeigt, dass Zytoskelettproteine eine wichtige Rolle bei der Tumorentstehung des Leberzellkarzinoms spielen. Septin 6 (SEPT6) ist ein hochgradig evolutionär konserviertes GTP-bindendes Protein, das eine bedeutende Rolle bei der Regulierung verschiedener zellbiologischer Verhaltensweisen wie Aktindynamik, Zellform und Zellmigration usw. spielt. Die Rolle von SEPT6 bei der Entwicklung des hepatozellulären Karzinoms (HCC) und der Hippo-Signalweg ist jedoch noch unbekannt. In dieser Studie haben wir die Rolle von SEPT6 beim hepatozellulären Karzinom und den zugrunde liegenden Mechanismus aufgedeckt.

Um die Rolle von SEPT6 auf HCC zu untersuchen, haben wir die Expression von SEPT6 in 30 Paaren von HCC-Proben mittels qRT-PCR gemessen. Die Expression von SEPT6 im HCC und in angrenzenden Nicht-Tumorgeweben wurde ebenfalls durch Western Blot bestätigt. Wir analysierten dann die Expression von SEPT6 in der GEPIA-Datenbank, wobei das Ergebnis auch die Hochregulation des SEPT6-mRNA-Spiegels in HCC-Geweben bestätigte. Als nächstes haben wir die Expression von SEPT6 in zwei normalen Leberzelllinien und mehreren HCC-Zelllinien gemessen. Zusammengenommen deuten diese Ergebnisse darauf hin, dass die SEPT6-Expression in HCC-Geweben und Zelllinien mit hochgradig metastatischem Potenzial hochreguliert ist.

Um die Rolle von SEPT6 bei der zellulären Funktion des HCC wie HCC-Proliferation, Zellzyklusprogression, Migration und Invasion zu untersuchen, haben wir Funktionsverlust- und Gewinn-Assays durchgeführt. Der erfolgreiche stabile SEPT6-Knockdown in MHCC-97H-Zellen und die Überexpression in Huh7-Zellen wurden durch qRT-PCR und Western Blot bestätigt. Um die Rolle von SEPT6 bei der Zellproliferation zu untersuchen, führten wir die CCK-8-Tests durch. Um zu untersuchen, ob SEPT6 die Proliferation durch Beeinflussung des Zellzyklusübergangs reguliert, haben wir die Zellzyklusverteilung mittels FACS nachgewiesen. Die Daten legten nahe, dass SEPT6 den G1/S-Zellzyklusübergang in HCC-Zellen fördert. In der Folge entdeckten wir die Expression von Cyclin D1 und Cyclin E1, die signifikant mit dem G1/S-Zellzyklusübergang zusammenhängen. Wir führten dann Transwell-Assays durch und untersuchten die Expression von MMP2 und MMP9 mittels qRT-PCR und WB, um die Migrations- und Invasionsfähigkeit von HCC-Zellen nach dem Knockdown oder der Überexpression von SEPT6 zu beurteilen. Schließlich fanden wir in vitro heraus, dass die Überexpression von SEPT6 die Proliferation, Zellzyklusprogression, Migration und Invasion von HCC-Zellen förderte, während die Unterdrückung von SEPT6 die entgegengesetzten

Auswirkungen auf die HCC-Zelllinien hatte. Daher gehen wir davon aus, dass SEPT6 beim HCC als Onkogen fumgiert, was im Gegensatz zu seiner Rolle bei Prostatakrebs steht.

Als nächstes untersuchten wir den zugrunde liegenden Mechanismus, warum SEPT6 als Onkogen wirkt. Wir konzentrierten uns hauptsächlich auf den Hippo-Signalweg, da dieser eine entscheidende Rolle bei der Tumorentstehung und -progression des HCC spielt. Unsere Daten bewiesen, dass die SEPT6-Überexpression den Hippo-Signalweg inaktivierte, den nachgeschalteten Effektor YAP stabilisierte, woraufhin das aktive YAP in den Zellkern translozierte, wo es die Transkription von Cyclin D1 und MMP2 förderte, was zu HCC-Wachstum und Metastasierung führte. Darüber hinaus verringerte der Knockdown von YAP die günstige Rolle von SEPT6 bei der HCC-Progression, während die YAP-Überexpression die hemmende Rolle der SEPT6-Abwärtsregulierung rettete. Mechanistisch gesehen übte SEPT6 seine onkogene Rolle beim HCC aus, indem es den Hippo /YAP-Signalweg regulierte.

Zusammenfassend lässt sich sagen, dass unsere Studie darauf hinweist, dass SEPT6 im HCC hochreguliert ist und als Onkogen in der HCC-Progression wirkt. Wir definierten, dass SEPT6 die HCC-Proliferation, die Migration und die Invasion im Zellzyklus fördert, was zumindest durch eine neue SEPT6/ Hippo /YAP-Achse erreicht wird. Insgesamt zeigten unsere Ergebnisse eine onkogene Rolle von SEPT6 beim HCC, die ein therapeutisches Interventionsziel für die Behandlung des HCC darstellen könnte.

Veröffentlichung 2:

Vorbehandlung mit Zink schützt Kupfferzellen nach Verabreichung von mikrobiellen Produkten

Zink ist ein essentielles Spurenmetall im menschlichen Körper und spielt eine wichtige Rolle bei der Zusammensetzung und Funktion von mehr als 300 Enzymen. Zink hat antioxidative und antiapoptotische Wirkungen und wird häufig in Studien gegen bakterielle Krankheitserreger verwendet. Systemische Entzündungen und schwere Fibrosen können zu einer signifikanten Senkung des Zinkspiegels im Serum führen, während eine Zinksupplementierung die Prognose von Patienten mit chronischer Lebererkrankung (CLD) verbessern könnte. Obwohl über zinkbezogene Behandlungen als neue antibakterielle Waffen berichtet wurde, gibt es noch keinen Konsens über die Dosierung, den Zeitpunkt und die Mechanismen, die für solche Effekte verantwortlich sind. In dieser Studie wurden humane primäre nicht-parenchymale Leberzellen [einschließlich KCs, HSZs und sinusoidale Endothelzellen (SECs)] mit Bakterienisolaten behandelt, die aus Stämmen von SBP-Patienten isoliert wurden. Durch die Kombination der von uns von 2016 bis 2019 gesammelten klinischen Daten wollten wir den Mechanismus von Zink zur Verhinderung mikrobieller Infektionen und seine klinische Anwendung bei Patienten mit CLD untersuchen.

Nach den Serum-Zinkspiegeln wurden 149 CLD-Patienten in 3 Gruppen eingeteilt. Die mit der Infektion und Fibrose verbundenen Marker wurden verglichen. Die Daten zeigten eine signifikant negative Korrelation zwischen den Serum-Zinkspiegeln und dem CRP und eine signifikant positive Korrelation zwischen Serum-Zink und Albumin in beiden Gruppen.

In In-vitro-Experimenten wurden mikrobielle Isolate von Patienten verwendet, um nicht-parenchymale Zellen der menschlichen Leber zu stimulieren, und in bestimmten Experimenten wurde die Zinksulfatlösung hinzugefügt. Durch den Vergleich der Wirkung von Zink durch LDH- und Thromboxan-A2-Spiegel im Zellüberstand wollten wir die klinische Anwendung von Serum-Zink bei Patienten mit CLD und seinen anti-infektiven Mechanismus in in-vitro-Studien untersuchen. Wir fanden heraus, dass eine Vorbehandlung mit Zink die Verletzung der bakteriellen Stimulation bei TMCs schützen könnte. Patienten mit niedrigen Serumzinkwerten zeigten im Vergleich zu anderen Gruppen höhere C-reaktive Proteine (CRP), GGT, INR, Gesamtbilirubin, MELD-Score und niedrigere Albuminwerte. CRP und Albumin waren sowohl in den Niedrig- als auch in den Normalzinkgruppen signifikant mit dem Serumzink korreliert. Bakterienisolate erhöhten die LDH-Spiegel in Kupfferzellen (KCs) und hepatischen Sternzellen signifikant, hatten aber keinen Einfluss auf Sinusendothelzellen, während die Vorbehandlung mit Zink zwar die KCs, nicht aber die hepatischen Sternzellen schützte.

Schließlich untersuchten wir den möglichen verwandten Pfad für den Zinkschutz durch RT-qPCR und stellten fest, dass der Myd88-verwandte Pfad für die schützende Wirkung der Zink-Vorbehandlung bei bakteriell induzierten Verletzungen in KCs wesentlich ist, und dass die verminderte Produktion von Thromboxan A2 auf die verminderte Genexpression von Myd88, MAPK und NF-kB zurückzuführen ist.

Zusammenfassend lässt sich sagen, dass die Serum-Zink-Konzentration ein wertvoller Marker für die Beurteilung des Schweregrades der Infektion und der Leberfibrose bei Patienten mit CLD sein kann. Darüber hinaus vertiefen unsere Ergebnisse unser Verständnis der Zinksupplementierung als antimikrobielle Waffe: Die Vorbehandlung mit Zink reduziert die Entzündung durch Hemmung der Aktivierung des Myd88-MAPK-NF-κB-Signalwegs bei KCs und TXA2 als wichtigen Akteur.

7 Publication 1 (pdf)

SEPT6 drives hepatocellular carcinoma cell proliferation, migration and invasion via the Hippo/YAP signaling pathway. Int J Oncol. 2021 Jun;58(6):25.
doi: 10.3892/ijo.2021.5205. Epub 2021 Apr 13.

Yuhui Fan, Zhipeng Du, Qiang Ding, Jiang Zhang, Mark op den Winkel, Alexander L. Gerbes, Mei Liu, Christian J. Steib

SEPT6 drives hepatocellular carcinoma cell proliferation, migration and invasion via the Hippo/YAP signaling pathway

YUHUI FAN[1], ZHIPENG DU[2], QIANG DING[2], JIANG ZHANG[1], MARK OP DEN WINKEL[1], ALEXANDER L. GERBES[1], MEI LIU[2] and CHRISTIAN J. STEIB[1]

[1]Department of Medicine II, Liver Center Munich, University Hospital, Ludwig-Maximilians-University of Munich, Munich 81377, Germany; [2]Department of Gastroenterology, Institute of Liver and Gastrointestinal Diseases, Tongji Hospital, Tongji Medical College, Huazhong University of Science and Technology, Wuhan, Hubei 430030, P.R. China

Received October 8, 2020; Accepted March 8, 2021

DOI: 10.3892/ijo.2021.5205

Abstract. Septin 6 (SEPT6) is a member of the GTP-binding protein family that is highly conserved in eukaryotes and regulates various biological functions, including filament dynamics, cytokinesis and cell migration. However, the functional importance of SEPT6 in hepatocellular carcinoma (HCC) is not completely understood. The present study aimed to investigate the expression levels and roles of SEPT6 in HCC, as well as the underlying mechanisms. The reverse transcription quantitative PCR, western blotting and immunohistochemistry staining results demonstrated that SEPT6 expression was significantly elevated in HCC tissues compared with corresponding adjacent non-tumor tissues, which indicated that SEPT6 expression may serve as a marker of poor prognosis for HCC. By performing plasmid transfection and G418 treatment, stable SEPT6-knockdown and SEPT6-overexpression cell lines were established. The Cell Counting Kit-8, flow cytometry and Transwell assay results demonstrated that SEPT6 overexpression significantly increased HCC cell proliferation, cell cycle transition, migration and invasion compared with the Vector group, whereas SEPT6 knockdown displayed significant suppressive effects on HCC cell lines *in vitro* compared with the control group. Mechanistically, SEPT6 might facilitate F-actin formation, which induced large tumor suppressor kinase 1 dephosphorylation, inhibited Hippo signaling, upregulated yes-associated protein (YAP) expression and nuclear translocation, and upregulated cyclin D1 and matrix metallopeptidase 2 (MMP2) expression. Furthermore, YAP overexpression significantly reversed SEPT6 knockdown-induced inhibitory effects on HCC, whereas YAP knockdown significantly inhibited the oncogenic effect of SEPT6 overexpression on HCC. Collectively, the present study demonstrated that SEPT6 may promote HCC progression by enhancing YAP activation, suggesting that targeting SEPT6 may serve as a novel therapeutic strategy for HCC.

Correspondence to: Dr Christian J. Steib, Department of Medicine II, Liver Center Munich, University Hospital, Ludwig-Maximilians-University of Munich, 15 Marchioninistrasse, Munich 81377, Germany
E-mail: fyhmed@yeah.net; christian.steib@med.uni-muenchen.de

Dr Mei Liu, Department of Gastroenterology, Institute of Liver and Gastrointestinal Diseases, Tongji Hospital, Tongji Medical College, Huazhong University of Science and Technology, 1095 Jiefang Avenue, Qiaokou, Wuhan, Hubei 430030, P.R. China
E-mail: tjliumei@yeah.net

Key words: hepatocellular carcinoma, septin 6, proliferation, migration, invasion, Hippo/yes-associated protein signaling pathway

Introduction

In 2018, hepatocellular carcinoma (HCC) was estimated to be the sixth most common cancer and the third most common cause of cancer-related mortality, resulting in ~841,000 new cases and 781,000 deaths worldwide (1,2). Although advances in therapeutic strategies have benefited patients who are diagnosed at an early stage, the majority of patients with HCC are diagnosed at an advanced stage and their overall survival remains poor, which is primarily attributed to the recurrence and metastasis of the disease (3). Therefore, identifying novel causative genes and molecular mechanisms underlying HCC progression is important for the development of therapeutic targets with improved efficacy.

Recent studies revealed that the Hippo signaling pathway is implicated in tumorigenesis and may display tumor suppressor effects (4-6). The core of Hippo signaling consists of macrophage stimulating 1/2, which regulates activation of large tumor suppressor kinase 1/2 (LATS1/2). Active LATS1/2 phosphorylates the downstream transcriptional co-activator Yes-associated protein (YAP)/tafazzin (TAZ). In the cytoplasm, the proteasome mediates ubiquitination and degradation of phosphorylated YAP/TAZ, which suppresses the transcription of proliferation- and survival-associated genes (7). Increasing evidence has indicated that the Hippo signaling pathway is crucial for HCC initiation and progression (8-10). Several factors have been reported to regulate Hippo signaling, including actin cytoskeleton, cell polarity and cell contact (11). Moreover, recent studies have demonstrated that cytoskeletal proteins regulate HCC progression by activating the Hippo signaling pathway (6,12,13).

Septins are highly conserved GTP-binding proteins family incorporating 13 members, which are ubiquitously expressed in the majority of eukaryotes (14). Recently, septins were categorized as the fourth cytoskeletal component, which interacts with cellular membranes, actin filaments and microtubules, and regulates various cellular processes (15). Among the 13 members, septin 6 (SEPT6) primarily regulates filament dynamics, cytokinesis, proliferation, cell cycle transition, survival and chemotaxis (14,16-18). In prostate cancer tissues, SEPT6 expression was decreased, and SEPT6 knockdown contributed to prostate cancer survival and invasion (18). Recently, it was reported that SEPT6 expression was upregulated in liver fibrosis, which promoted hepatic stellate cell activation, proliferation and migration (19). A previous study demonstrated that Hepatitis B surface antigen (HBsAg) knockdown blocked HCC growth, whereas HBsAg knockdown decreased SEPT6 expression in HepG2.2.15 cells (20), indicating that SEPT6 may be involved in HCC pathogenesis. However, the functional importance of SEPT6 in HCC development and the regulation of the Hippo signaling pathway is not completely understood.

The present study aimed to investigate whether SEPT6 expression was upregulated in HCC tissues and to determine its association with prognosis. The effects of SEPT6 overexpression on HCC cell proliferation, cell cycle transition, migration and invasion, and the role of the Hippo signaling pathway and YAP activation were investigated. The results of the present study may indicate a novel therapeutic strategy for HCC.

Materials and methods

HCC samples and cell lines. A total of 64 patients (51 male patients and 13 female patients; age range, 26-78 years; average age, 52.58±12.73) were enrolled in the present study at Tongji Hospital (Wuhan, China) between January 2011 and December 2014. The inclusion criteria were as follows: i) Patients were pathologically diagnosed with HCC; ii) patients underwent surgical excision; and iii) patients were aged >18 years. The exclusion criteria were as follows: i) Patients received preoperative therapy; and ii) patients with more than one primary tumor. The tumor and corresponding adjacent non-tumor (distance from tumor margin, >2 cm) tissues were collected. Tissues were fixed with 4% paraformaldehyde at room temperature for 48 h, embedded in paraffin and sectioned to 5-μm thick sections for immunohistochemistry staining. Alternatively, tissues were immediately preserved at -80˚C for RNA and protein extraction. The clinicopathological characteristics of the patients were recorded, including sex, age, hepatitis B virus infection, α-fetoprotein levels, tumor size, tumor number and metastasis (Table I). Written informed consent was obtained from all patients. The present study was approved by the Ethics Committee of Tongji Hospital (approval no. TJ-IRB20180404) and was conducted according to the principles outlined in the Declaration of Helsinki. Two normal hepatocyte cell lines (THLE-2 and THLE-3), Hep3B and Huh7 were purchased from American Type Culture Collection. MHCC-97L and MHCC-97H were purchased from The Cell Bank of Type Culture Collection of The Chinese Academy of Sciences. HCC-LM3 was obtained from the Liver Cancer Institute, Zhongshan Hospital, Fudan University (Shanghai, China). Cells were cultured in DMEM supplemented with 10% FBS (Gibco; Thermo Fisher Scientific, Inc.), 100 U/ml penicillin and 100 μg/ml streptomycin at 37˚C with 5% CO_2.

Reagent. The F-actin inhibitor latrunculin B (Lat. B) was purchased from Abcam (cat. no. ab144291) and was used following the standard protocol. Briefly, latrunculin B (1 mg) was dissolved in 40 μl DMSO to make a 25 mg/ml stock solution. The stock solution was stored at -20˚C until subsequent use. Before use, Lat. B was thawed and added to DMEM to a final concentration of 10 μM. Cells were treated with Lat. B for 2 h at 37˚C.

Reverse transcription-quantitative PCR (RT-qPCR). Total RNA extraction, reverse transcription, and RT-qPCR were performed following a standard protocol, as previously described (19). Total RNA was extracted from liver tissues and cell lines using TRIzol® reagent (Invitrogen; Thermo Fisher Scientific, Inc.). RNA concentrations were determined using a NanoDrop 2000 Spectrophotometer (Thermo Fisher Scientific, Inc.). Total RNA was reverse transcribed into cDNA using the PrimeScript reagent kit (Takara Biotechnology Co., Ltd.) according to the manufacturer's protocol. The following temperature protocol was used for reverse transcription: 37˚C for 15 min and 85˚C for 5 sec. Subsequently, qPCR was performed using SYBR Premix ExTaq (Takara Biotechnology Co., Ltd.) and an ABI StepOne Real-Time PCR System (Applied Biosystems; Thermo Fisher Scientific, Inc.) according to the manufacturer's protocol. The following thermocycling conditions were used for qPCR: Pre-denaturation at 95˚C for 30 sec; followed by 40 cycles of 95˚C for 5 sec and 60˚C for 30 sec. mRNA expression levels were quantified using the $2^{-\Delta\Delta Cq}$ method (21) and normalized to the internal reference gene β-actin. The sequences of the primers used for qPCR are presented in Table SI.

Western blotting and co-immunoprecipitation (co-IP). Total protein was extracted from liver tissues and cell lines using RIPA buffer containing protease inhibitors PMSF and cocktail (Servicebio Technology Co., Ltd.). Nuclear proteins were extracted using NE-PER (Thermo Fisher Scientific, Inc.). Protein concentrations were determined using a BCA kit (Boster Biological Technology). Western blotting was performed as previously described (19). Briefly, proteins (30 μg per lane) were separated via 10% SDS-PAGE and transferred onto PVDF membranes (EMD Millipore), which were then blocked with 5% BSA (cat. no. 4240GR100; Guangzhou Saiguo Biotech Co., Ltd.) at room temperature for 1 h. Subsequently, the membranes were incubated with primary antibodies at 4˚C overnight. After washing three times in TBST, the membranes were incubated with HRP-conjugated secondary antibodies (Beyotime Institute of Biotechnology) at room temperature for 1 h. After washing three times, protein bands were detected using an ECL assay kit (Advansta, Inc.). Protein expression was semi-quantified using ImageJ software (version 1.44p; National Institutes of Health) with β-actin as the loading control. The primary and secondary antibodies used for western blotting are listed in Table SII.

Table I. Association between SEPT6 expression and clinicopathological variables in human HCC tissues.

	SEPT6 expression		
Variable	Low (n=18)	High (n=46)	P-value
Sex			0.530
Female	4	9	
Male	14	37	
Age (years)			0.578
≤45	6	16	
>45	12	30	
HBsAg			0.291
Negative	5	18	
Positive	13	28	
AFP (ng/ml)			0.172
≤400	8	13	
>400	10	33	
Tumor diameter (cm)			0.010[a]
≤5	11	12	
>5	7	34	
Tumor number			0.490
Single	13	35	
Multiple	5	11	
Metastasis			0.016[a]
No	11	13	
Yes	7	33	

SEPT6 expression was assessed via reverse transcription-quantitative PCR. SEPT6 high/low expression indicated that SEPT6 expression in was higher/lower in HCC tissues compared with corresponding adjacent non-tumor tissues. [a]P<0.05. SEPT6, septin 6; HCC, hepatocellular carcinoma; HBsAg, hepatitis B surface antigen; AFP, α-fetoprotein.

For the co-IP assay, MHCC-97H cells (2-5x10^7) were washed twice with cold PBS twice and lysed using 1% NP-40 buffer (cat. no. P0013F; Beyotime Institute of Biotechnology) containing protease inhibitors at 4˚C for 30 min. After centrifugation at 12,000 x g for 15 min at 4˚C, the supernatant was collected. Protein A/G PLUS-Agarose beads (cat. no. sc-2003; Santa Cruz Biotechnology, Inc.) were washed three times with PBS and diluted in PBS to 50% concentration. Subsequently, the Agarose beads (100 μl/ml) were added to the supernatant (containing 200-600 μg protein). The mixture was incubated for 30 min at 4˚C on a horizontal shaker. After centrifugation at 1,000 x g for 5 min at 4˚C, the supernatant was collected and divided into two parts. SEPT6 antibody (2 μg/500 μg cell lysate) or isotype normal IgG antibody (2 μg/500 μg cell lysate; cat. no. sc-2026; Santa Cruz Biotechnology, Inc.) was added to the supernatant (~500 μl total volume) and incubated for 1 h at 4˚C. Subsequently, additional Agarose beads (100 μl/ml) were added and incubated at 4˚C overnight. After centrifugation at 1,000 x g for 5 min at 4˚C, the supernatant was discarded and the pellets were washed four times with 1.0 ml NP-40 buffer. The samples were boiled with sample loading buffer for 10 min, and the Agarose beads were discarded. The supernatant was collected and analyzed via western blotting using antibodies targeted against SEPT6, LATS1 and LATS2 according to the aforementioned protocol. The antibodies used for co-IP are listed in Table SII.

Immunohistochemistry (IHC) staining. The expression of SEPT6 in HCC samples and corresponding adjacent non-tumor tissues were analyzed by IHC, as previously described (19). Briefly, paraffin-embedded slides were de-paraffinized in xylene and rehydrated using an alcohol gradient. Antigen retrieval was performed by heating samples in 0.01 mol/l citrate buffer (pH 6.0) for 15 min in a microwave. Subsequently, the slides were immersed in 3% H_2O_2 at room temperature for 15 min to eliminate the endogenous peroxidase. After washing three times with PBS, the sections were blocked using 10% goat serum (Boster Biological Technology) at room temperature for 30 min. Subsequently, the sections were incubated with an anti-SEPT6 (cat. no. 12805-1-AP; 1:100; ProteinTech Group, Inc.) at 4˚C overnight. After washing three times with PBS, the sections were incubated with a biotinylated secondary antibody (cat. no. SP-9000; OriGene Technologies, Inc.) at 37˚C for 1 h. After washing three times with PBS, peroxidase activity was visualized using DAB (OriGene Technologies, Inc.) at room temperature for ~10 sec. Then, the sections were counterstained with hematoxylin (OriGene Technologies, Inc.) at room temperature for ~1 min. Stained samples were visualized using an IX71 light microscope (Olympus Corporation; magnification, x100).

Immunofluorescence staining. Huh7 cells (5x10^4 each well) were seeded onto glass cover slides in 24-well plates overnight. Subsequently, cells were fixed with 4% formaldehyde at room temperature for 20 min, permeabilized using 0.3% Triton X-100 and blocked with 5% BSA (cat. no. 4240GR100; BioFroxx; Saiguo Biological Technology Co., Ltd.) at room temperature for 30 min. Subsequently, the slides were incubated with ActinRed (cat. no. KGMP0012; Nanjing KeyGen Biotech Co., Ltd.) at room temperature for 20 min. The nuclei were counterstained with DAPI solution (cat. no. G1012; Wuhan Servicebio Technology Co., Ltd.) at room temperature for 10 min. Stained cells were observed using an IX71 fluorescence microscope (Olympus Corporation; magnification, x400).

Plasmid transfection and stable cell line selection. The plasmids used for SEPT6 and YAP knockdown and overexpression were purchased from Shanghai GeneChem Co., Ltd. At 80-90% confluence, cells were transfected with 2 μg plasmid using Lipofectamine® 3000 (Invitrogen; Thermo Fisher Scientific, Inc.) in Opti-MEM (Gibco; Thermo Fisher Scientific, Inc.) according to the manufacturer's protocol. At 6-8 h post-transfection, the cell culture medium was replaced with DMEM supplemented with 10% FBS. The control shRNA was a non-targeting shRNA and the overexpression control was an empty vector. The shRNA sequences are presented in Table SI. At 48 h post-transfection, transfected cell lines were treated with G418 (400 μg/ml) for 2 weeks to select stably transfected cells. Transfection efficiencies were assessed and the stable cell lines were used for subsequent experiments. The following cell lines were established: MHCC-97H-shcontrol,

MHCC-97H-shSEPT6, Huh7-Vector, Huh7-SEPT6, MHCC-97H-shSEPT6+YAP, Huh7-SEPT6+shYAP, HCC-LM3-shcontrol, HCC-LM3-shSEPT6, Hep3B-Vector and Hep-3B-SEPT6.

Cell Counting Kit-8 (CCK-8) assay. Cell proliferation was detected using the CCK-8 kit (cat. no. C0037; Beyotime Institute of Biotechnology) according to the manufacturer's protocol, as previously described (19). Briefly, cells were seeded ($1x10^3$ cells/well) into 96-well plates and cultured for 24, 48, 72 or 96 h. Subsequently, the culture medium was replaced with 100 μl DMEM and 10 μl CCK-8. After incubation for 2 h, the absorbance of each well was measured at a wavelength of 450 nm using an ELISA reader.

Flow cytometry analysis of the cell cycle. Cell cycle distribution was assessed by flow cytometry, as previously described (22). Briefly, cells ($1x10^6$) were harvested, washed with cold PBS and fixed using 75% ethanol overnight at 4˚C. After washing twice with PBS, cells were incubated with PI staining solution containing RNase (cat. no. KGA511-KGA512; Nanjing KeyGen Biotech Co., Ltd.) at 37˚C for 30 min in the dark. Subsequently, cell cycle distribution was analyzed using a BD FACSVerse flow cytometer (BD Biosciences) and CELLQuestPro software (version 5.1; BD Biosciences).

Transwell assays. Transwell insert chambers (pore size, 8 μm; Corning, Inc.) were used to examine cell invasion and migration, respectively. For the invasion assay, the upper chamber inserts were precoated with Matrigel (BD Biosciences) at 37˚C for 1 h. Briefly, 200 μl serum-free DMEM containing cells ($2x10^4$) was plated into the upper chamber and the lower chamber was filled with 600 μl DMEM supplemented with 20% FBS. Following incubation at 37˚C for 24 h, migratory/invading cells were fixed using absolute methanol at room temperature for 10 min, and stained using 0.2% crystal violet solution at room temperature for 1 h. Cells were observed using an IX71 microscope (Olympus Corporation; magnification, x100) in at least three fields of view.

Database. The Gene Expression Profiling Interactive Analysis (GEPIA) database (gepia.cancer-pku.cn) was used to determine SEPT6 mRNA expression levels in human liver HCC specimens and corresponding adjacent non-tumor specimens.

Statistical analysis. Each experiment was performed in triplicate. Data are presented as the mean ± SD. Statistical analyses were performed using GraphPad Prism (version 5.0; GraphPad Software, Inc.) or SPSS (version 19.0; IBM Corp.) software. Comparisons between two groups were analyzed using the paired or unpaired Student's t-test. Comparisons among multiple groups were analyzed using one-way ANOVA followed by Tukey's post hoc test. Categorical data were analyzed using Fisher's exact test. Patient survival was analyzed via Kaplan-Meier analysis and log-rank tests. $P<0.05$ was considered to indicate a statistically significant difference.

Results

SEPT6 is upregulated in human HCC and predicts poor prognosis. To examine SEPT6 expression in HCC, SEPT6 mRNA expression levels were assessed in 64 paired HCC samples. Compared with corresponding adjacent non-tumor samples, SEPT6 mRNA expression levels were significantly higher in 46 paired HCC samples (71.88%; Fig. 1A). Subsequently, we selected 20 paired tissues, including 16 paired tissues with higher SEPT6 mRNA expression in the HCC tisues compared with the adjacent non-tumor tissues, and 4 paired tissues with lower SEPT6 mRNA expression in HCC tissues compared with the adjacent non-tumor tissues. The protein expression levels of SEPT6 were determined via western blotting. The results demonstrated that the protein expression levels of SEPT6 were significantly higher in 16 HCC tissues compared with the adjacent non-tumor tissues (Fig. 1B and S1A, C and D), whereas the protein expression levels of SEPT6 were significantly lower in 4 HCC tissues compared with the adjacent non-tumor tissues (Fig. S1B), indicating a positive association between mRNA and protein expression levels of SEPT6 in human patients with HCC. The association between SEPT6 expression levels and clinicopathological characteristics was investigated. SEPT6 expression levels were significantly associated with tumor size and metastasis, but not significantly associated with sex, age, hepatitis B virus infection, tumor number or α-fetoprotein levels (Table I). Furthermore, the association between SEPT6 expression and overall survival was assessed. SEPT6 high/low expression represented that SEPT6 expression in the HCC tissues was higher/lower compared with the corresponding adjacent non-tumor tissues (fold change >1.5), respectively. The results demonstrated that high SEPT6 expression levels indicated significantly worse overall survival in patients with HCC compared with low SEPT6 expression levels (Fig. 1C). IHC staining demonstrated that SEPT6 expression levels were notably higher in HCC samples compared with corresponding adjacent non-tumor samples, and SEPT6 protein expression was primarily localized in the cytoplasm (Fig. 1D). In addition, analysis of the GEPIA database demonstrated significantly upregulated SEPT6 expression in HCC compared with adjacent non-tumor tissues (Fig. 1E). Subsequently, SEPT6 expression levels were examined in two normal hepatocyte cell lines (THLE-2 and THLE-3) and several HCC cell lines. Among HCC cell lines, MHCC-97H and HCC-LM3 cells display the highest metastatic potential (23-25). The results suggested that SEPT6 expression was significantly higher in the majority of the HCC cell lines, particularly in those with high metastatic potential (MHCC-97H and HCC-LM3), compared with normal hepatocytes (Fig. 1F and G). Collectively, the results indicated that SEPT6 expression was upregulated in human HCC and may serve as a predictor of poor prognosis.

SEPT6 promotes HCC cell proliferation. Subsequently, gain- and loss-of-function assays were performed to assess the effect of SEPT6 on HCC cell function. Following assessment of SEPT6 endogenous expression levels in different HCC cells, MHCC-97H and Huh7 cells were selected for SEPT6 knockdown or overexpression, respectively, and stably transfected cells were established. Transfection efficiencies were determined by measuring SEPT6 mRNA and protein expression levels (Fig. 2A and C). The CCK-8 assay results indicated that SEPT6 knockdown significantly inhibited MHCC-97H cell proliferation compared with the control group, whereas SEPT6

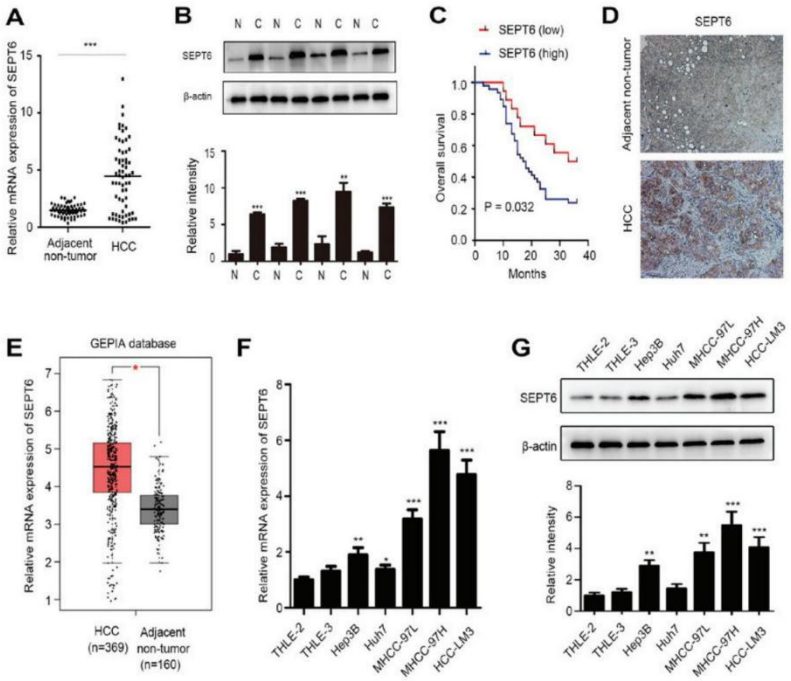

Figure 1. SEPT6 is upregulated in human HCC and predicts poor prognosis. (A) SEPT6 mRNA expression levels in 64 paired HCC samples and adjacent non-tumor tissues were assessed via RT-qPCR. (B) SEPT6 protein expression levels in HCC samples (n=4) and corresponding adjacent non-tumor samples (n=4) were assessed via western blotting. (C) Association between SEPT6 expression and overall survival as determined by Kaplan-Meier survival analysis. SEPT6 low expression (n=18) and SEPT6 high expression (n=46). (D) SEPT6 staining in HCC samples and corresponding adjacent non-tumor samples (magnification, x100). (E) SEPT6 expression in HCC and corresponding adjacent non-tumor samples derived from the GEPIA database. SEPT6 (F) mRNA and (G) protein expression levels in the normal hepatocyte cell lines and HCC cell lines were determined via RT-qPCR and western blotting, respectively. *P<0.05, **P<0.01 and ***P<0.001 vs. N or THLE2. SEPT6, septin 6; HCC, hepatocellular carcinoma; RT-qPCR, reverse transcription-quantitative PCR; GEPIA, Gene Expression Profiling Interactive Analysis; N, adjacent non-tumor tissues; C, HCC tissues.

overexpression significantly increased Huh7 cell proliferation compared with the Vector group (Fig. 2B). Subsequently, flow cytometry was performed to investigate whether SEPT6 regulated the cell cycle. Compared with the control group, SEPT6 knockdown resulted in significantly increased cell cycle arrest at the G_1/S phase in MHCC-97H cells, but displayed no significant effect on the G_2/M transition (Fig. 2D). By contrast, compared with the Vector group, SEPT6 overexpression significantly promoted G_1/S transition in Huh7 cells, but had no significant effect on G_2/M transition. The results suggested that SEPT6 primarily regulated the G_1/S transition, whereas its effect on the G_2/M transition was not significant. Furthermore, cyclin D1 and cyclin E1 expression levels are significantly associated with G_1/S cell cycle transition (15). The RT-qPCR results indicated that SEPT6 knockdown significantly decreased cyclin D1 expression in MHCC-97H cells compared with the control group, whereas SEPT6 overexpression significantly increased cyclin D1 expression in Huh7 cells compared with the Vector group (Fig. 2E). However, cyclin E1 mRNA expression levels were not significantly altered by SEPT6 knockdown or overexpression compared with the control and Vector groups, respectively. Consistent results were obtained for protein expression levels (Fig. 2F). Collectively, the results indicated that SEPT6 promoted HCC cell proliferation and G_1/S transition *in vitro*.

SEPT6 promotes HCC cell migration and invasion. Metastasis is the leading cause of HCC-related mortality (26). The Transwell assay results demonstrated that SEPT6 knockdown significantly decreased MHCC-97H cell migration and invasion compared with the control group, whereas SEPT6 overexpression significantly increased Huh7 cell migration and invasion compared with the Vector group (Fig. 3A and B). Moreover, matrix metallopeptidase (MMP)2 expression levels were significantly decreased by SEPT6 knockdown in MHCC-97H cells compared with the control group, whereas SEPT6 overexpression significantly increased MMP2 expression levels in Huh7 cells compared with the Vector group (Fig. 3C). However, MMP9 mRNA expression levels were not significantly altered in response to SEPT6 knockdown or overexpression compared

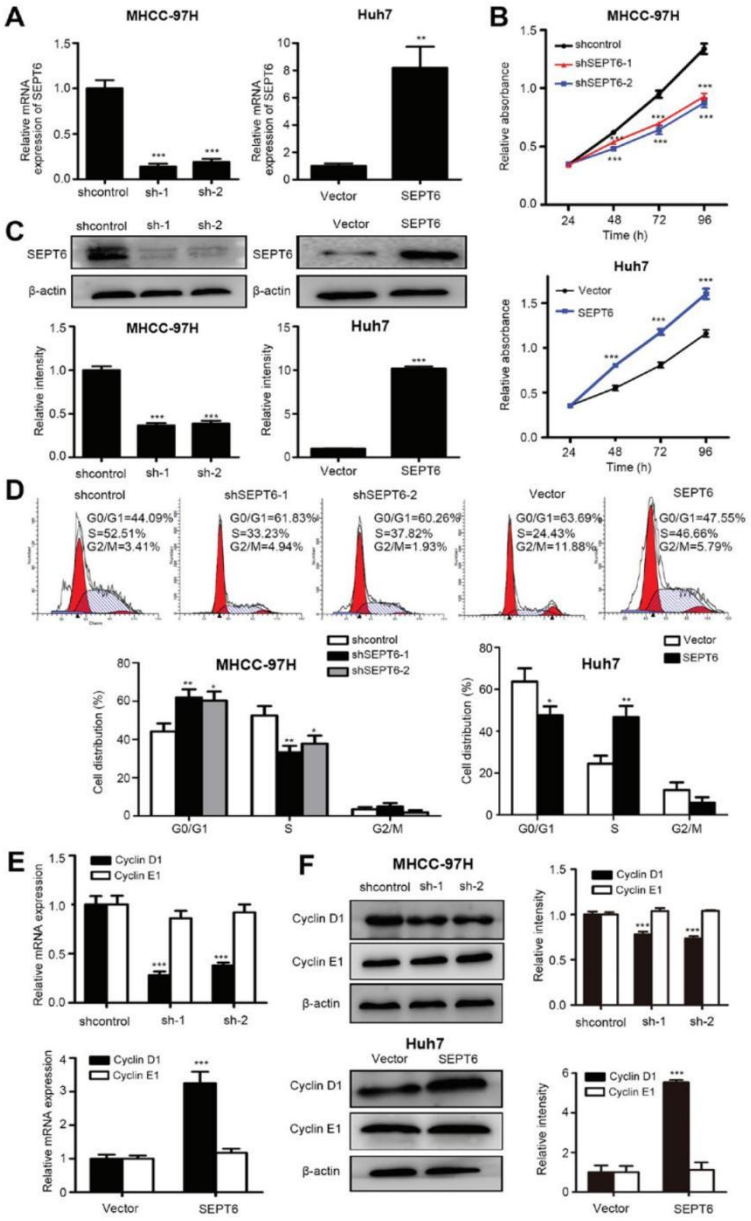

Figure 2. SEPT6 promotes HCC cell proliferation. SEPT6-knockdown MHCC-97H and SEPT6-overexpression Huh7 cells were established by transfection with the corresponding plasmids. At 48 h post-transfection, cells were treated with G418 (400 μg/ml) for 2 weeks for stable cell selection. (A) Transfection efficiencies were determined via RT-qPCR. (B) Cell Counting Kit-8 assays were performed to assess cell proliferation. (C) Transfection efficiencies were also determined via western blotting. (D) Flow cytometry was conducted to analyze cell cycle distribution. Cyclin D1 and cyclin E1 (E) mRNA and (F) protein expression levels were measured via RT-qPCR and western blotting, respectively. *P<0.05, **P<0.01 and ***P<0.001 vs. shcontrol or Vector. SEPT6, septin 6; HCC, hepatocellular carcinoma; RT-qPCR, reverse transcription-quantitative PCR; sh, short hairpin RNA.

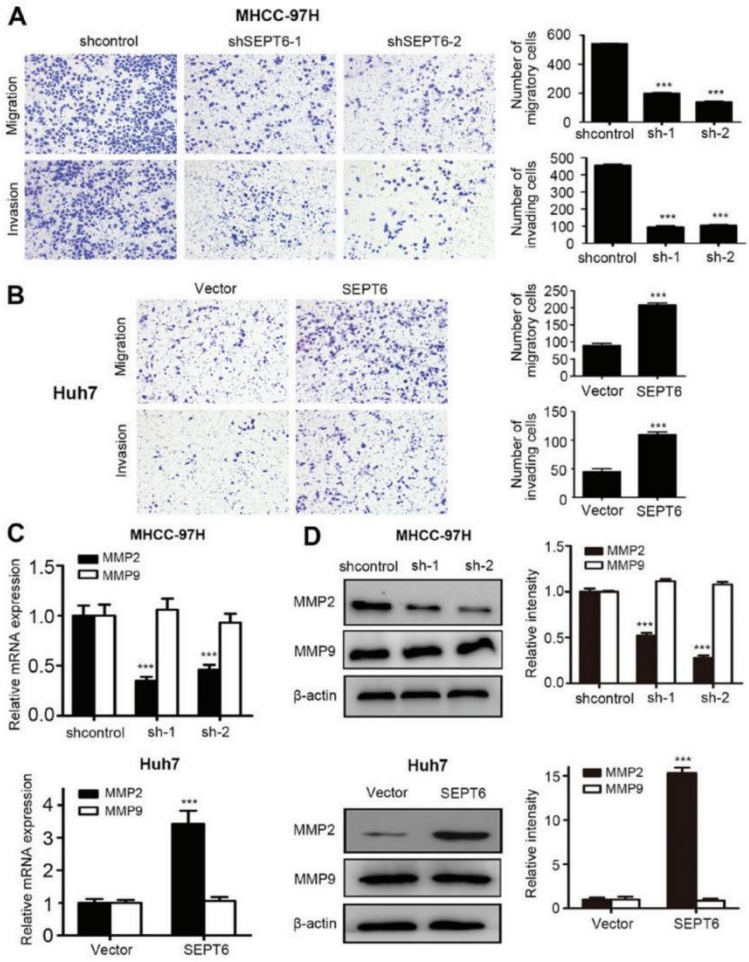

Figure 3. SEPT6 promotes HCC cell migration and invasion. Transwell assays were conducted to assess (A) MHCC-97H and (B) Huh7 cell migration and invasion (magnification, x100). MMP2 and MMP9 (C) mRNA and (D) protein expression levels were measured via reverse transcription-quantitative PCR and western blotting, respectively. ***P<0.001 vs. shcontrol or Vector. SEPT6, septin 6; HCC, hepatocellular carcinoma; MMP, matrix metallopeptidase; sh, short hairpin RNA.

with the control and Vector groups, respectively (Fig. 3C). Similar results were obtained via western blotting (Fig. 3D). Collectively, the *in vitro* results demonstrated that SEPT6 enhanced HCC cell migration and invasion.

SEPT6 regulates the Hippo/YAP signaling pathway in HCC. As aforementioned, SEPT6 promoted HCC cell proliferation and migration; therefore, the mechanism underlying its action was investigated. Increasing evidence has demonstrated that Hippo signaling is crucial for HCC tumorigenesis and metastasis (8-10). Furthermore, Hippo signaling is primarily regulated by the actin cytoskeleton (11). Septin proteins are considered as the fourth cytoskeletal component and SEPT6 regulates actin cytoskeleton dynamics (15); therefore, the present study further investigated whether SEPT6 promoted HCC cell progression by regulating Hippo signaling. The transfection efficiency of SEPT6 knockdown and overexpression in HCC-LM3 and Hep3B cells, respectively, was verified via RT-qPCR and western blotting (Fig. S2). The western blotting results indicated that compared with the control group, SEPT6 knockdown significantly promoted the phosphorylation of LATS1 and YAP in MHCC-97H and HCC-LM3 cells, but notably decreased the overall expression of YAP. By contrast, compared with the vector group, SEPT6

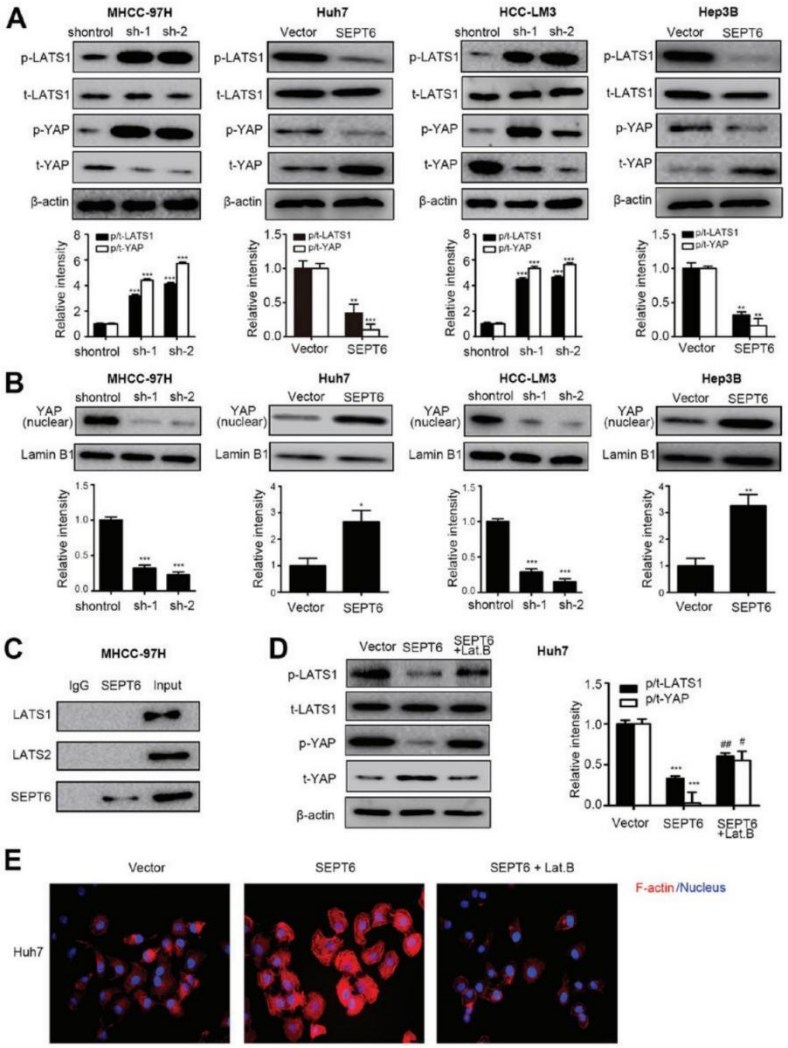

Figure 4. SEPT6 regulates the Hippo/YAP signaling pathway in HCC. (A) p-LATS1, LATS1, p-YAP and YAP protein expression levels were measured via western blotting. (B) Nuclear YAP protein expression levels were measured via western blotting using Lamin B1 as the loading control. (C) Co-immunoprecipitation assays were performed to determine the interaction between SEPT6 and LATS1 or LATS2. SEPT6-overexpression Huh7 cells were treated with 10 μM Lat. B for 2 h to disrupt the cytoskeleton. (D) Protein expression levels of p-LATS1, LATS1, p-YAP and YAP were measured via western blotting. (E) F-actin formation was determined by performing immunofluorescence assays (magnification, x400). *P<0.05, **P<0.01 and ***P<0.001 vs. shcontrol or Vector; $^{\#}$P<0.05 and $^{\#\#}$P<0.01 vs. SEPT6. SEPT6, septin 6; YAP, yes-associated protein; HCC, hepatocellular carcinoma; p, phosphorylated; LATS1, large tumor suppressor kinase 1; Lat. B, Latrunculin B; t, total; sh, short hairpin RNA.

overexpression significantly decreased the phosphorylation of LATS1 and YAP, and markedly increased the overall expression of YAP both in Huh7 and Hep3B cells (Fig. 4A). The results indicated that SEPT6 may regulate the activity of Hippo signaling, while modulating the activity, stability and overall expression of YAP. Subsequently, the present study examined whether SEPT6 regulated YAP nuclear translocation. The western blotting results demonstrated that SEPT6 knockdown significantly decreased nuclear YAP protein expression levels in MHCC-97H and HCC-LM3 cells compared with the

control group, whereas SEPT6 overexpression significantly upregulated nuclear YAP protein expression levels in Huh7 and Hep3B cells compared with the Vector group (Fig. 4B). The results suggested that SEPT6 upregulation may inactivate Hippo signaling by inhibiting the phosphorylation of LATS1, which resulted in inhibition of YAP phosphorylation, as well as proteasome-induced YAP ubiquitination and degradation. Therefore, higher protein expression levels of YAP were translocated to the nucleus, resulting in enhanced gene transcription.

Furthermore, an endogenous co-IP assay was performed to investigate whether SEPT6 interacted with LATS1 and LATS2. The results indicated that SEPT6 did not directly interact with LATS (Fig. 4C). Septins, the fourth component of the cytoskeleton, lack the kinase activity domain (6); therefore, SEPT6 may regulate LATS1 phosphorylation indirectly, which may be associated with the cytoskeleton-regulating function of the septin proteins. To verify this hypothesis, SEPT6-overexpression Huh7 cells were treated with the F-actin inhibitor Lat. B to disrupt the cytoskeleton. Subsequently, F-actin levels and the phosphorylated and overall expression levels of LATS1 and YAP were assessed. The results indicated that compared with the vector group, SEPT6 overexpression notably facilitated F-actin formation, which was markedly disrupted by Lat. B (Fig. 4E). Furthermore, Lat. B treatment increased LATS1 and YAP phosphorylation, thus notably decreasing YAP overall expression in SEPT6-overexpression Huh7 cells (Fig. 4D). Collectively, the results indicated that SEPT6 may regulate Hippo/YAP signaling in HCC by modulating F-actin formation.

SEPT6 regulates HCC cell proliferation, cell cycle progression, migration and invasion via the Hippo/YAP signaling pathway. The present study further investigated whether SEPT6 exerted its effects via regulating the Hippo/YAP signaling pathway. Firstly, the transfection efficiencies of YAP-overexpression plasmids in MHCC-97H cells and YAP-knockdown plasmids in Huh7 cells were verified by measuring mRNA and protein expression levels, which suggested that these plasmids were appropriate for YAP overexpression and knockdown (Fig. S3). Subsequently, YAP was overexpressed by plasmid transfection in stable SEPT6-knockdown MHCC-97H cells and stable cells were selected by G418. YAP upregulation in MHCC-97H-shSEPT6 cells was validated by protein expression analysis (Fig. 5A). Compared with the control group, SEPT6 knockdown significantly decreased MHCC-97H cell proliferation, G_1/S transition, migration and invasion (Fig. 5B-D). SEPT6 knockdown-induced effects were significantly reversed by YAP overexpression. YAP downregulation was achieved by shRNA transfection in stable SEPT6-overexpression Huh7 cells, and stable cells were selected for further experiments. YAP knockdown was verified in Huh7-SEPT6 cells (Fig. 5E). Compared with the Vector group, SEPT6 overexpression significantly enhanced Huh7 cell proliferation, migration, invasion and G_1/S phase transition (Fig. 5F-H). SEPT6 overexpression-mediated effects were significantly reversed by YAP knockdown. Furthermore, the present study assessed whether YAP was involved in SEPT6-regulated cyclin D1 and MMP2 expression. YAP overexpression significantly upregulated cyclin D1 and MMP2 expression levels in SEPT6-knockdown MHCC-97H cells, whereas YAP knockdown significantly decreased cyclin D1 and MMP2 expression levels in SEPT6-overexpression Huh7 cells (Fig. 5I). Furthermore, to analyze SEPT6-independent effects of YAP on the regulation of cyclin D1 and MMP2 expression, four stable cell lines were established by plasmid transfection and G418 selection using Huh7 cells, namely Huh7-Vector, Huh7-SEPT6, Huh7-shYAP and Huh7-shYAP-SEPT6. Compared with the Vector group, SEPT6 overexpression significantly upregulated cyclin D1 and MMP2 expression levels, whereas YAP knockdown not only inhibited SEPT6-mediated effects on cyclin D1 and MMP2 expression, but also significantly decreased cyclin D1 and MMP2 expression levels (Fig. S4). Collectively, the results demonstrated that the Hippo/YAP signaling axis may serve a key role in SEPT6-induced HCC cell proliferation, cell cycle progression, migration and invasion.

Discussion

HCC is the third leading cause of cancer-related mortality, and its prognosis is extremely poor due to early relapse and metastasis following curative resection (3). Although various therapeutic targets have been identified, the prognosis of patients with HCC remains poor (3). To the best of our knowledge, the present study was the first to demonstrate that SEPT6 inhibited Hippo signaling, activated the downstream effector YAP, and enhanced cyclin D1 and MMP2 expression levels, which promoted HCC growth and metastasis.

SEPT6 is primarily implicated in hematological malignancies (27), nervous system development (16) and tumor progression (18). In prostate cancer, SEPT6 expression is downregulated, and SEPT6 knockdown promotes cancer cell survival and invasion, suggesting a tumor suppressor role (18). However, the present study demonstrated that SEPT6 expression was significantly increased in HCC tissues compared with corresponding adjacent non-tumor tissues, which was associated with poor prognosis. The results prompted investigation into why SEPT6 expression was upregulated in HCC tissues. It was hypothesized that the malignant transformation of tumor cells and the complicated tumor microenvironment, which involves hypoxia, inflammatory cytokines stimulation, metabolic reprogramming and epigenetic regulation, might be the leading causes for SEPT6 upregulation in HCC. Moreover, the leading cause of HCC and whether the causes work synergistically requires further investigation. SEPT6 overexpression significantly enhanced HCC cell proliferation, cell cycle transition, migration and invasion compared with the Vector group, whereas SEPT6 knockdown displayed the opposite effects compared with the control group. Therefore, SEPT6 was identified as an oncogene in HCC, which contrasted to its role in prostate cancer. It was previously reported that SEPT6 promoted liver fibrogenesis (19). Since liver fibrosis and liver cirrhosis are considered as the precancerous states of HCC, it is reasonable to hypothesize that SEPT6 may promote HCC progression. The results of the present study indicated that the expression patterns and effects of SEPT6 in prostate cancer and HCC were opposite, which may be due to different genetic backgrounds, including gene mutation, or the tumor microenvironment. The roles of certain proteins are context-dependent; therefore, the difference in the tumor

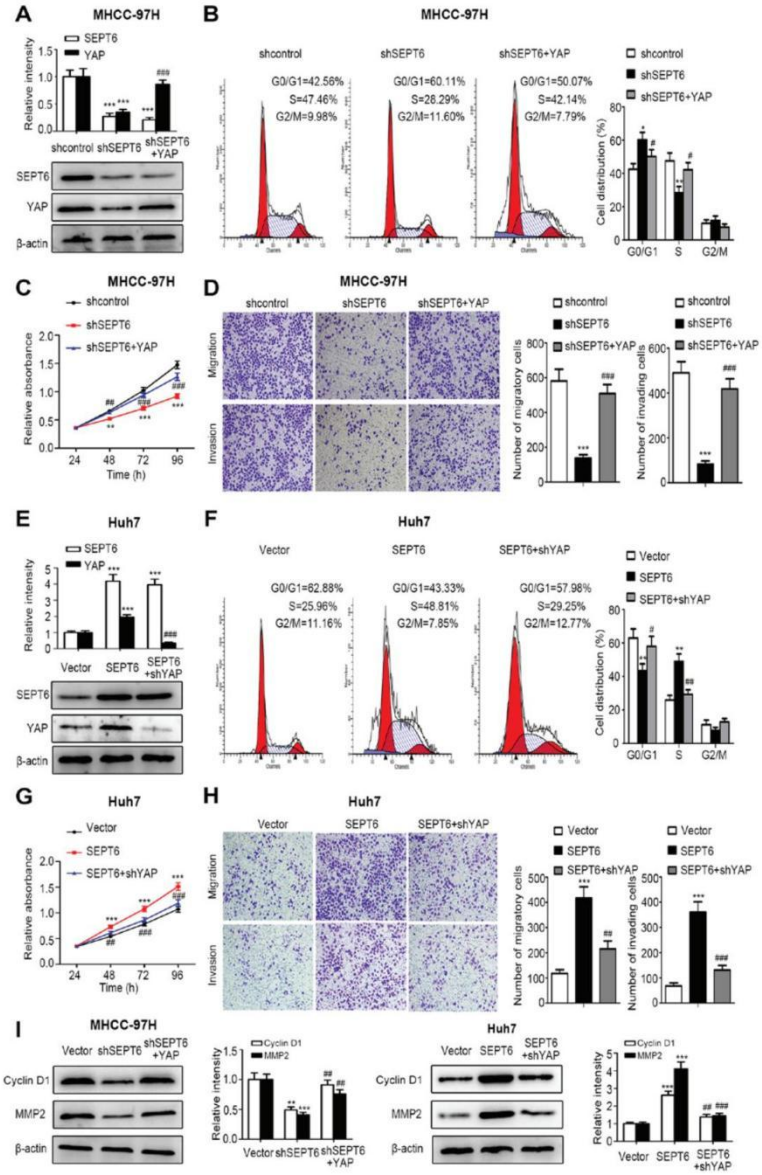

Figure 5. SEPT6 regulates HCC cell proliferation, cell cycle progression, migration and invasion via the Hippo/YAP signaling pathway. MHCC-97H-shSEPT6 cells were transfected with YAP and stable Huh7-SEPT6 cells were transfected with shYAP. Subsequently, G418 was used for stable cell selection. (A) Transfection efficiencies of shSEPT6 and YAP were determined via western blotting. MHCC-97H cell (B) cycle distribution, (C) proliferation, (D) migration and invasion (magnification, x100) were assessed by performing CCK-8, flow cytometry and Transwell assays, respectively. (E) Transfection efficiencies of SEPT6 and shYAP were determined via western blotting. Huh7 cell (F) cycle distribution, (G) proliferation, (H) migration and invasion (magnification, x100) were assessed by performing CCK-8, flow cytometry and Transwell assays, respectively. (I) Cyclin D1 and MMP2 protein expression levels were determined via western blotting. *P<0.05, **P<0.01 and ***P<0.001 vs. Vector; #P<0.05, ##P<0.01 and ###P<0.001 vs. shSEPT6 or SEPT6. SEPT6, septin 6; HCC, hepatocellular carcinoma; YAP, yes-associated protein; sh, short hairpin RNA; CCK-8, Cell Counting Kit-8; MMP2, matrix metallopeptidase 2.

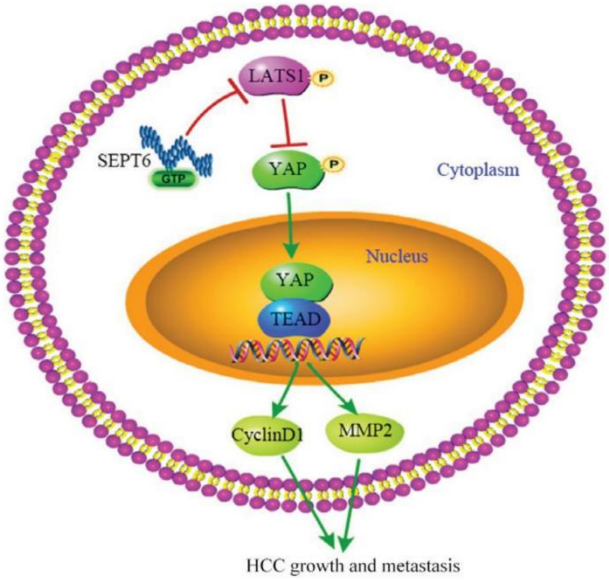

Figure 6. Summary of SEPT6-regulated Hippo/YAP signaling pathway in HCC. SEPT6 expression was upregulated in HCC, which inactivated Hippo signaling, dephosphorylated and stabilized the downstream effector YAP and upregulated YAP expression. Subsequently, active YAP was translocated to the nucleus and promoted transactivation of cyclin D1 and MMP2, resulting in HCC cell proliferation and metastasis. SEPT6, septin 6; YAP, yes-associated protein; HCC, hepatocellular carcinoma; MMP2, matrix metallopeptidase 2; TEAD, TEA domain transcription factor; p, phosphorylated

microenvironment between HCC and prostate cancer may result in different expression patterns and functional roles of SEPT6.

Subsequently, the mechanism underlying the oncogenic action of SEPT6 was examined. The present study focused on the Hippo signaling pathway, which is crucial for HCC tumorigenesis and progression (8-10). Hippo signaling is primarily regulated by the actin cytoskeleton (11). For example, the cytoskeletal protein PDZ and LIM domain 1 inhibited HCC metastasis by activating Hippo signaling (6). SEPT6 has been reported to regulate actin and microtubule remodeling (17). Based on the aforementioned studies, the potential role of SEPT6 in promoting HCC progression in a Hippo/YAP-dependent manner was assessed. The results indicated that compared with the Vector group, SEPT6 overexpression inactivated Hippo signaling, and dephosphorylated and stabilized the downstream effector YAP, leading to the translocation of active YAP into the nucleus and the transactivation of cyclin D1 and MMP2, which resulted in HCC cell proliferation and metastasis (Fig. 6). Furthermore, YAP knockdown significantly reversed the oncogenic effects of SEPT6 overexpression on HCC progression, whereas YAP overexpression significantly reversed SEPT6 knockdown-mediated inhibitory effects. As previously reported, YAP regulates cyclin D1 and MMP2 expression independently, regardless of SEPT6 expression (26,28-30). The results of the present study also demonstrated that YAP knockdown inhibited SEPT6-mediated upregulation of cyclin D1 and MMP2 expression. The results demonstrated that SEPT6 regulated cyclin D1 and MMP2 expression via YAP, and YAP independently regulated cyclin D1 and MMP2 expression to a certain extent.

The regulatory mechanism underlying Hippo signaling has received increasing attention. Hippo signaling can be regulated by mechanical force, the extracellular matrix, cell-cell contact and cytoskeletal interactions (7,11,31,32). With regard to cytoskeletal interactions, Hippo signaling can be regulated by F-actin levels, F-actin activity and cytoskeletal tension (11). In HCC cell lines, F-actin was confirmed to bind to LATS1, resulting in the dephosphorylation and inactivation of Hippo signaling (6). Furthermore, the Rho GTPase serves an important role in regulating Hippo signaling activity by the cytoskeleton (31). Septins belong to a family of GTP-binding proteins and are considered as the fourth cytoskeletal component. In addition, SEPT6 was reported to regulate actin cytoskeleton dynamics (14,15). Based on previous studies, it was hypothesized that SEPT6 may regulate Hippo via three possible mechanisms, one of which involves the regulation of F-actin formation by SEPT6 in order to affect cytoskeleton dynamics. Subsequently, F-actin binds to LATS1 and causes Hippo inactivation. The hypothesis was confirmed by the present study, since compared with the Vector group, SEPT6 overexpression notably facilitated F-actin formation, whereas disruption of F-actin by Lat. B abrogated SEPT6-induced LATS1 dephosphorylation and Hippo inactivation. Furthermore, whether SEPT6 regulates other proteins associated with cytoskeleton dynamics, including Ezrin and neurofibromin 2 (NF2), requires further investigation. Previous

studies reported that Ezrin and NF2 were involved in the regulation of Hippo signaling (33,34). Secondly, as a GTP-binding protein, SEPT6 may regulate GTPase activity and thus, Hippo signaling activity. Finally, it may be possible that SEPT6 mediates the recruitment of certain phosphatases to repress LATS1 phosphorylation. Collectively, the results of the present study indicated a possible mechanism by which SEPT6 regulated Hippo signaling via upregulation of F-actin formation. However, further investigation of the underlying mechanism is required.

In conclusion, the present study demonstrated that SEPT6 was upregulated in HCC and displayed an oncogenic function in HCC progression. SEPT6 promoted HCC cell proliferation, cell cycle progression, migration and invasion, which was mediated at least partly via the SEPT6/Hippo/YAP axis. Therefore, the results of the present study may provide novel insight into HCC treatment.

Acknowledgements

Not applicable.

Funding

The present study was supported by the Deutsche Forschungsgemeinschaft (grant nos. DFG STE 1022/2-3 and DFG STE 1022/4-1), the National Natural Science Foundation of China (grant nos. 81272657 and 81572422) and the China Scholarship Council (grant nos. 201908080017 and 201606230249).

Availability of data and materials

The datasets used and/or analyzed during the present study are available from the corresponding author upon reasonable request.

Authors' contributions

YF performed the cytologic and mechanistic experiments. ZD and QD analyzed the data. JZ analyzed the clinical data. QD and JZ confirm the authenticity of all the raw data. MODW and ALG made substantial contributions to the conception of the study and drafted the manuscript. ML and CJS designed the study and revised the manuscript. All authors read and approved the final manuscript.

Ethics approval and consent to participate

The present study was approved by the Tongji Hospital Ethics Committee (approval no. TJ-IRB20180404). Written informed consent was obtained from each patient in accordance with the ethical standards of the World Medical Association Declaration of Helsinki.

Patient consent for publication

Not applicable.

Competing interests

The authors declare that they have no competing interests.

References

1. Yang JD, Hainaut P, Gores GJ, Amadou A, Plymoth A and Roberts LR: A global view of hepatocellular carcinoma: Trends, risk, prevention and management. Nat Rev Gastroenterol Hepatol 16: 589-604, 2019.
2. Bray F, Ferlay J, Soerjomataram I, Siegel RL, Torre LA and Jemal A: Global cancer statistics 2018: GLOBOCAN estimates of incidence and mortality worldwide for 36 cancers in 185 countries. CA Cancer J Clin 68: 394-424, 2018.
3. Kanwal F and Singal AG: Surveillance for hepatocellular carcinoma: Current best practice and future direction. Gastroenterology 157: 54-64, 2019.
4. Ji S, Liu Q, Zhang S, Chen Q, Wang C, Zhang W, Xiao C, Li Y, Nian C, Li J, *et al*: FGF15 activates Hippo signaling to suppress bile acid metabolism and liver tumorigenesis. Dev Cell 48: 460-474.e9, 2019.
5. Dent P, Booth L, Roberts JL, Liu J, Poklepovic A, Lalani AS, Tuveson D, Martinez J and Hancock JF: Neratinib inhibits Hippo/YAP signaling, reduces mutant K-RAS expression, and kills pancreatic and blood cancer cells. Oncogene 38: 5890-5904, 2019.
6. Huang Z, Zhou JK, Wang K, Chen H, Qin S, Liu J, Luo M, Chen Y, Jiang J, Zhou L, *et al*: PDLIM1 inhibits tumor metastasis through activating Hippo signaling in hepatocellular carcinoma. Hepatology 71: 1643-1659, 2020.
7. Meng Z, Moroishi T and Guan KL: Mechanisms of Hippo pathway regulation. Genes Dev 30: 1-17, 2016.
8. Zhou D, Conrad C, Xia F, Park JS, Payer B, Yin Y, Lauwers GY, Thasler W, Lee JT, Avruch J, *et al*: Mst1 and Mst2 maintain hepatocyte quiescence and suppress hepatocellular carcinoma development through inactivation of the Yap1 oncogene. Cancer Cell 16: 425-438, 2009.
9. Feng X, Lu T, Li J, Yang R, Hu L, Ye Y, Mao F, He L, Xu J, Wang Z, *et al*: The tumor suppressor interferon regulatory factor 2 binding protein 2 regulates Hippo pathway in liver cancer by a feedback loop in mice. Hepatology 71: 1988-2004, 2020.
10. Li Y, Lu J, Chen Q, Han S, Shao H, Chen P, Jin Q, Yang M, Shangguan F, Fei M, *et al*: Artemisinin suppresses hepatocellular carcinoma cell growth, migration and invasion by targeting cellular bioenergetics and Hippo-YAP signaling. Arch Toxicol 93: 3367-3383, 2019.
11. Sun S and Irvine KD: Cellular organization and cytoskeletal regulation of the Hippo signaling network. Trends Cell Biol 26: 694-704, 2016.
12. Chen Q, Zhou XW, Zhang AJ and He K: ACTN1 supports tumor growth by inhibiting Hippo signaling in hepatocellular carcinoma. J Exp Clin Cancer Res 40: 23, 2021.
13. Yang XM, Cao XY, He P, Li J, Feng MX, Zhang YL, Zhang XL, Wang YH, Yang Q, Zhu L, *et al*: Overexpression of Rac GTPase activating protein 1 contributes to proliferation of cancer cells by reducing Hippo signaling to promote cytokinesis. Gastroenterology 155: 1233-1249.e22, 2018.
14. Longtine MS, DeMarini DJ, Valencik ML, Al-Awar OS, Fares H, De Virgilio C and Pringle JR: The septins: Roles in cytokinesis and other processes. Curr Opin Cell Biol 8: 106-119, 1996.
15. Mostowy S and Cossart P: Septins: The fourth component of the cytoskeleton. Nat Rev Mol Cell Biol 13: 183-194, 2012.
16. Hu J, Bai X, Bowen JR, Dolat L, Korobova F, Yu W, Baas PW, Svitkina T, Gallo G and Spiliotis ET: Septin-driven coordination of actin and microtubule remodeling regulates the collateral branching of axons. Curr Biol 22: 1109-1115, 2012.
17. Kremer BE, Adang LA and Macara IG: Septins regulate actin organization and cell-cycle arrest through nuclear accumulation of NCK mediated by SOCS7. Cell 130: 837-850, 2007.
18. Wei Y, Yang J, Yi L, Wang Y, Dong Z, Liu Z, Ou-yang S, Wu H, Zhong Z, Yin Z, *et al*: MiR-223-3p targeting SEPT6 promotes the biological behavior of prostate cancer. Sci Rep 4: 7546, 2014.
19. Fan Y, Du Z, Steib CJ, Ding Q, Lu P, Tian D and Liu M: Effect of SEPT6 on the biological behavior of hepatic stellate cells and liver fibrosis in rats and its mechanism. Lab Invest 99: 17-36, 2019.
20. Xiangji L, Feng X, Qingbao C, Weifeng T, Xiaoqing J, Baihe Z, Feng S, Hongyang W and Mengchao W: Knockdown of HBV surface antigen gene expression by a lentiviral microRNA-based system inhibits HBV replication and HCC growth. J Viral Hepat 18: 653-660, 2011.
21. Livak KJ and Schmittgen TD: Analysis of relative gene expression data using real-time quantitative PCR and the 2(-Delta Delta C(T)) method. Methods 25: 402-408, 2001.

22. Kondo R, Ishino K, Wada R, Takata H, Peng WX, Kudo M, Kure S, Kaneya Y, Taniai N, Yoshida H, *et al*: Downregulation of protein disulfide isomerase A3 expression inhibits cell proliferation and induces apoptosis through STAT3 signaling in hepatocellular carcinoma. Int J Oncol 54: 1409-1421, 2019.
23. Li Y, Tang ZY and Hou JX: Hepatocellular carcinoma: Insight from animal models. Nat Rev Gastroenterol Hepatol 9: 32-43, 2011.
24. Sun F, Wang J, Sun Q, Li F, Gao H, Xu L, Zhang J, Sun X, Tian Y, Zhao Q, *et al*: Interleukin-8 promotes integrin β3 upregulation and cell invasion through PI3K/Akt pathway in hepatocellular carcinoma. J Exp Clin Cancer Res 38: 449, 2019.
25. Ding ZB, Shi YH, Zhou J, Shi GM, Ke AW, Qiu SJ, Wang XY, Dai Z, Xu Y and Fan J: Liver-intestine cadherin predicts microvascular invasion and poor prognosis of hepatitis B virus-positive hepatocellular carcinoma. Cancer 115: 4753-4765, 2009.
26. Xia H, Dai X, Yu H, Zhou S, Fan Z, Wei G, Tang Q, Gong Q and Bi F: EGFR-PI3K-PDK1 pathway regulates YAP signaling in hepatocellular carcinoma: The mechanism and its implications in targeted therapy. Cell Death Dis 9: 269, 2018.
27. Cerveira N, Bizarro S and Teixeira MR: MLL-SEPTIN gene fusions in hematological malignancies. Biol Chem 392: 713-724, 2011.
28. Pan Y, Tong JH, Lung RW, Kang W, Kwan JS, Chak WP, Tin KY, Chung LY, Wu F, Ng SS, *et al*: RASAL2 promotes tumor progression through LATS2/YAP1 axis of hippo signaling pathway in colorectal cancer. Mol Cancer 17: 102, 2018.
29. Zhang J, Xu ZP, Yang YC, Zhu JS, Zhou Z and Chen WX: Expression of Yes-associated protein in gastric adenocarcinoma and inhibitory effects of its knockdown on gastric cancer cell proliferation and metastasis. Int J Immunopathol Pharmacol 25: 583-590, 2012.
30. Xie K, Xu C, Zhang M, Wang M, Min L, Qian C, Wang Q, Ni Z, Mou S, Dai H, *et al*: Yes-associated protein regulates podocyte cell cycle re-entry and dedifferentiation in adriamycin-induced nephropathy. Cell Death Dis 10: 915, 2019.
31. Zhang C, Wang F, Gao Z, Zhang P, Gao J and Wu X: Regulation of Hippo signaling by mechanical signals and the cytoskeleton. DNA Cell Biol 39: 159-166, 2020.
32. Matsui Y and Lai ZC: Mutual regulation between Hippo signaling and actin cytoskeleton. Protein Cell 4: 904-910, 2013.
33. Xue Y, Bhushan B, Mars WM, Bowen W, Tao J, Orr A, Stoops J, Yu Y, Luo J, Duncan AW, *et al*: Phosphorylated Ezrin (Thr567) regulates Hippo pathway and yes-associated protein (Yap) in liver. Am J Pathol 190: 1427-1437, 2020.
34. Matsuda T, Zhai P, Sciarretta S, Zhang Y, Jeong JI, Ikeda S, Park J, Hsu CP, Tian B, Pan D, *et al*: NF2 activates Hippo signaling and promotes ischemia/reperfusion injury in the heart. Circ Res 119: 596-606, 2016.

Figure S1. SEPT6 protein expression levels in another 16 paired HCC and corresponding adjacent non-tumor tissue samples were assessed via western blotting. (A, C and D) SEPT6 protein expression levels were increased in 12 HCC tissues compared with the adjacent non-tumor tissues. (B) SEPT6 protein expression levels were decreased in 4 HCC tissues compared with the adjacent non-tumor tissues. $^{**}P<0.01$ and $^{***}P<0.001$ vs. corresponding adjacent non-tumor tissue samples. SEPT6, septin 6; HCC, hepatocellular carcinoma; N, adjacent non-tumor tissues; C, HCC tissues.

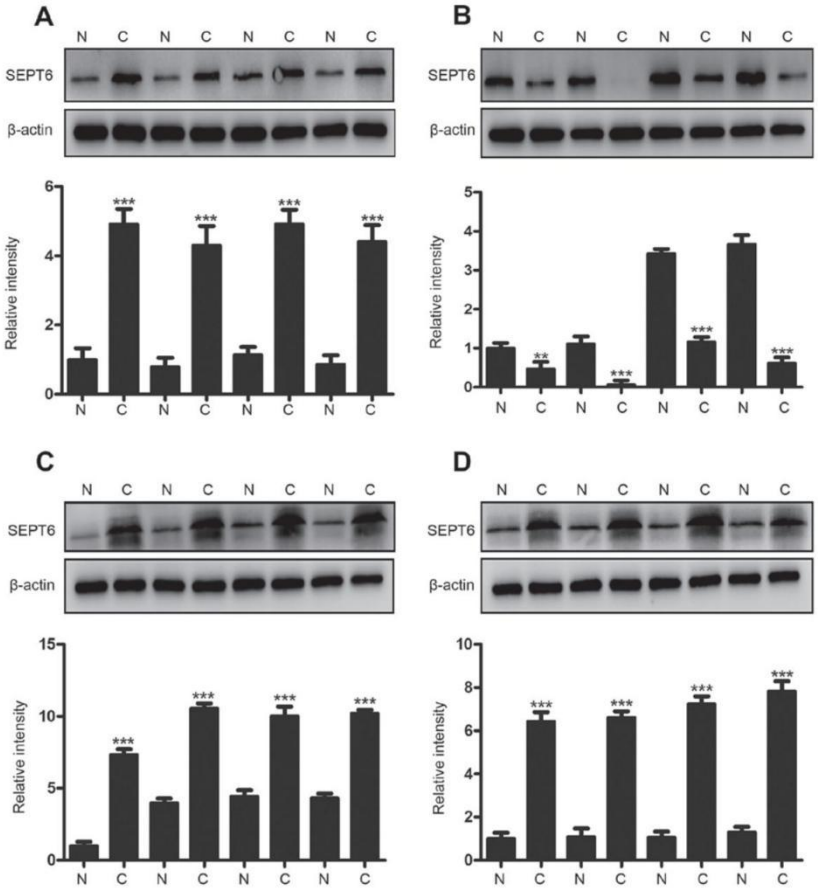

Figure S2. Transfection efficiencies of SEPT6 knockdown and overexpression. Transfection efficiencies of sh-SEPT61/2 in HCC-LM3 cells and SEPT6 in Hep3B cells were determined via (A) reverse transcription-quantitative PCR and (B) western blotting. At 48 h post-transfection, cells were treated with G418 (400 μg/ml) for 2 weeks for stable cell selection. **P<0.01 and ***P<0.001 vs. shcontrol or Vector. SEPT6, septin 6; sh, short hairpin RNA.

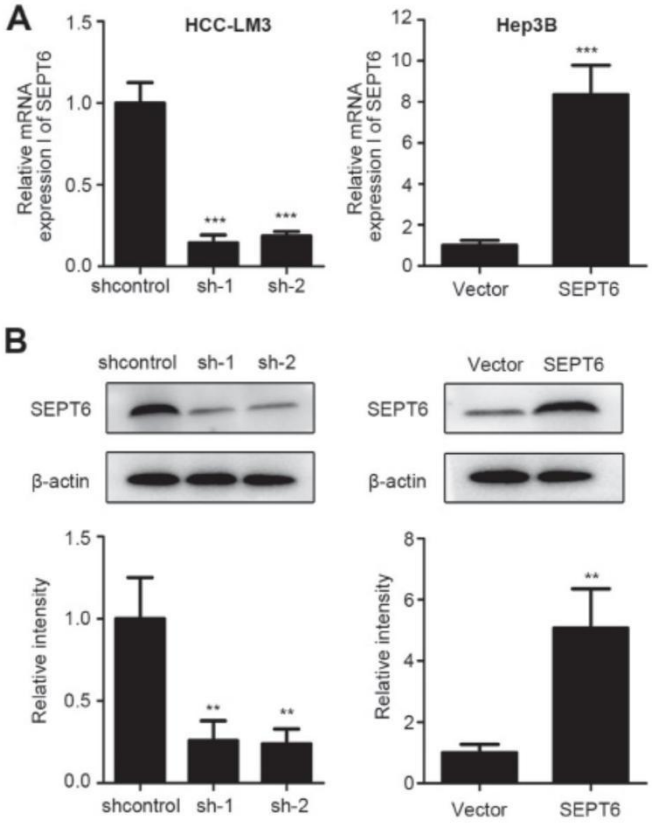

Figure S3. Transfection efficiency of YAP knockdown and overexpression. MHCC-97H cells were transfected with YAP or vector. Huh7 cells were transfected with sh-YAP or sh-control. At 48 h post-transfection, cells were treated with G418 (400 μg/ml) for 2 weeks for stable cell selection. Transfection efficiencies were determined via (A) reverse transcription-quantitative PCR and (B) western blotting. **P<0.01 and ***P<0.001 vs. Vector or shcontrol. YAP, yes-associated protein; sh, short hairpin RNA.

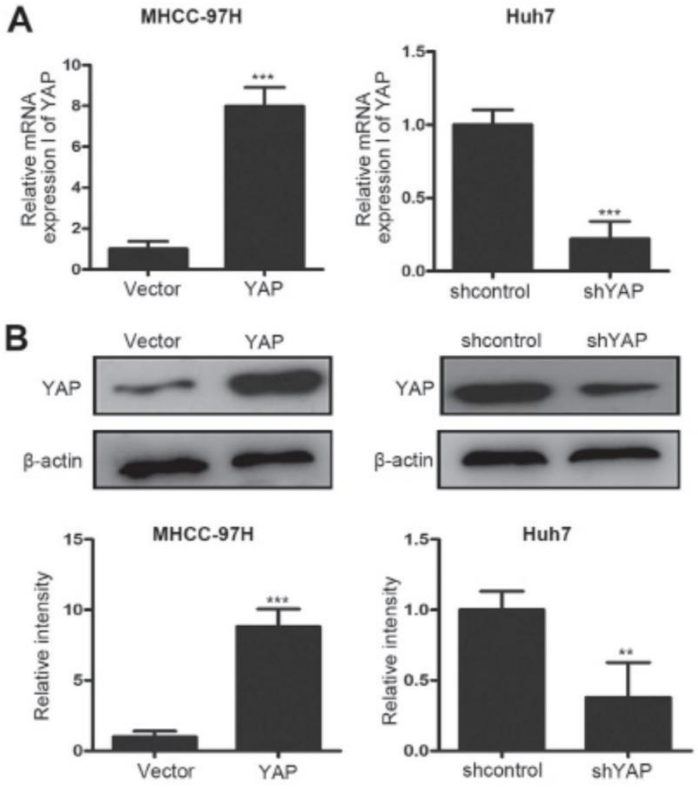

Figure S4. SEPT6 regulates cyclin D1 and MMP2 expression via YAP, and YAP also independently regulates cyclin D1 and MMP2 expression. Cyclin D1 and MMP2 (A) mRNA and (B) protein expression levels were determined via reverse transcription-quantitative PCR and western blotting. ***P<0.001 vs. Vector; ###P<0.001 vs. SEPT6. SEPT6, septin 6; MMP, matrix metallopeptidase; YAP, yes-associated protein; sh, short hairpin RNA

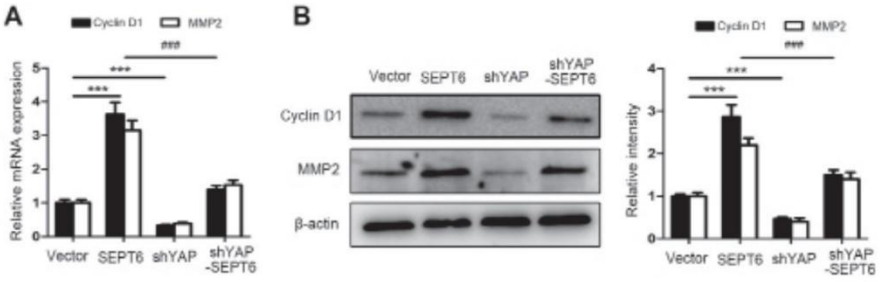

Table SI. Sequences of primers used for quantitative PCR and shRNAs.

Primer/vector	Sequence (5'→3')
β-actin	F: CATGTACGTTGCTATCCAGGC
	R: CTCCTTAATGTCACGCACGAT
SEPT6	F: TCCAAGAGAGCAACGTGAGG
	R: AATTCCACGATAGGCTTGTAGC
Cyclin D1	F: GCTGCGAAGTGGAAACCATC
	R: CCTCCTTCTGCACACATTTGAA
Cyclin E1	F: ACTCAACGTGCAAGCCTCG
	R: GCTCAAGAAAGTGCTGATCCC
MMP2	F: TACAGGATCATTGGCTACACACC
	R: GGTCACATCGCTCCAGACT
MMP9	F: TGTACCGCTATGGTTACACTCG
	R: GGCAGGGACAGTTGCTTCT
YAP	F: TAGCCCTGCGTAGCCAGTTA
	R: TCATGCTTAGTCCACTGTCTGT
shSEPT6-1	GCAGCACAGAAGAACUGAA
shSEPT6-2	GACCUAGUGACUAUGAAGA
shYAP	GGAATTGAGAACAATGACGAC
Control	UUCUCCGAACGUGUCACG

SEPT6, septin 6; MMP, matrix metallopeptidase; sh, short hairpin RNA; YAP, yes-associated protein; F, forward; R, reverse.

Table SII. Antibodies used for western blotting.

Antibody	Dilution	Cat. no.	Supplier details
SEPT6	1:400	12805-1-AP	ProteinTech Group, Inc.
Cyclin D1	1:2,000	60186-1-Ig	ProteinTech Group, Inc.
Cyclin E1	1:1,000	11554-1-AP	ProteinTech Group, Inc.
MMP2	1:1,000	4022	Cell Signaling Technology, Inc.
MMP9	1:300	BA0573	Boster Biological Technology Co., Ltd.
LATS1	1:1,000	9153	Cell Signaling Technology, Inc.
YAP	1:1,000	14074	Cell Signaling Technology, Inc.
p-LATS1	1:1,000	9157	Cell Signaling Technology, Inc.
p-YAP	1:1,000	13008	Cell Signaling Technology, Inc.
LATS2	1:1,000	5888	Cell Signaling Technology, Inc.
Lamin B1	1:5,000	66095-1-Ig	ProteinTech Group, Inc.
β-actin	1:2,000	BM0627	Boster Biological Technology Co., Ltd.
Anti-Rabbit IgG	1:1,000	A0208	Beyotime Institute of Biotechnology
Anti-mouse IgG	1:1,000	A0216	Beyotime Institute of Biotechnology

SEPT6, septin 6; MMP, matrix metallopeptidase; LATS, large tumor suppressor kinase; YAP, yes-associated protein; p, phosphorylated.

8 Publication 2 (pdf)

Pretreatment with Zinc protects Kupffer cells following administration of microbial products. Biomed Pharmacother. 2020 Jul;127:110208.
doi: 10.1016/j.biopha.2020.110208. Epub 2020 May 14.

Jiang Zhang, Andreas Wieser, Hao Lin, **Yuhui Fan**, Hanwei Li, Tobias S. Schiergens, Julia Mayerle, Alexander L. Gerbes, Christian J. Steib

Biomedicine & Pharmacotherapy 127 (2020) 110208

Contents lists available at ScienceDirect

Biomedicine & Pharmacotherapy

journal homepage: www.elsevier.com/locate/biopha

Pretreatment with zinc protects Kupffer cells following administration of microbial products

Jiang Zhang[a,b], Andreas Wieser[c,d,e], Hao Lin[a], Yuhui Fan[a], Hanwei Li[a], Tobias S. Schiergens[f], Julia Mayerle[a], Alexander L. Gerbes[a], Christian J. Steib[a,*]

[a] Department of Medicine II, University Hospital, Liver Centre Munich, LMU Munich, Germany
[b] Department of Liver Surgery and Liver Transplantation Center, Ren Ji Hospital, School of Medicine, Shanghai Jiao Tong University, Shanghai, China
[c] Medical Microbiology and Hospital Epidemiology, Max von Pettenkofer Institute, Faculty of Medicine, LMU Munich, Germany
[d] Division of Infectious Diseases and Tropical Medicine, University Hospital, LMU Munich, Germany
[e] German Center for Infection Research (DZIF), Partner Site Munich, 80802, Munich, Germany
[f] Department of General, Visceral, and Transplant Surgery, Ludwig-Maximilians-University Munich, Munich, Germany

ARTICLE INFO

Keywords:
Primary non-parenchymal cell
Spontaneous bacterial peritonitis
Zinc

ABSTRACT

Background: Systemic inflammation and severe fibrosis can reduce serum zinc levels, while zinc supplementation is reported to improve the prognosis of patients with chronic liver disease (CLD).
Objectives: We aimed to investigate the clinical application of serum zinc in patients with CLD and the anti-infective mechanism of zinc supplementation.
Methods: Based on the serum zinc level, 149 CLD patients were divided into 3 groups and their clinical parameters were compared. In *in-vitro* experiments, microbial isolates derived from patients were used to stimulate human liver non-parenchymal cells, and the zinc sulfate solution was added in certain experiments. The effect of zinc was compared by LDH and thromboxane A_2 levels in the cell supernatant.
Result: Compared with other groups, patients with low serum zinc levels had significantly higher C-reactive protein (CRP), total bilirubin, INR, creatinine, and MELD scores, while albumin and GOT levels were reduced. Only CRP and albumin were significantly correlated with serum zinc in both low and normal-zinc groups. Bacterial isolates significantly increased LDH levels in Kupffer cells (KCs) and stellate cells but had no effect on sinusoidal endothelial cells, whereas zinc pretreatment protected KCs but not stellate cells. Thromboxane A_2 secreted by KCs can also be induced by bacterial stimulation, accompanied by increased gene expression of Myd88, MAPK and NF-kB, while zinc pretreatment can attenuate that.
Conclusion: Serum zinc levels can be used to estimate infection and liver fibrosis in CLD patients. As a new antibacterial weapon, zinc supplementation acts on KCs through Myd88-MAPK related pathways.

1. Introduction

Zinc is an essential trace metal in the human body and plays an important role in the composition and function of more than 300 enzymes. The concentration of zinc in the plasma is about 15 μM, of which about 80 % is transported bound to albumin. Zinc has antioxidant and anti-apoptotic effects and is commonly used in studies against bacterial pathogens. Normally, zinc deficiency is due to inadequate dietary intake, but systemic inflammation also leads to a significant reduction in circulating zinc levels [1].

Chronic liver disease (CLD) is strongly associated with immune dysfunction that can lead to cirrhosis and serious complications [2]. Although the cause and mechanism from CLD to cirrhosis remain unclear, infection or inflammation may play an important role in this progression [3,4]. Thromboxane (TX) A_2 has been identified as an important effector of Kupffer cells (KCs) activated by bacteria and plays an important role in the progression of cirrhosis [5,6]. Zinc deficiency often leads to a reduction in the body's immune function and affects cirrhotic patients with clinical signs such as skin lesions, muscle spasms and hepatic encephalopathy [7]. Patients with zinc deficiency are more likely to develop spontaneous bacterial peritonitis (SBP) than patients with normal zinc levels, and ascites is an independent predictor of

Abbreviations: CLD, chronic liver disease; HSC, hepaticstellate cells; KC, Kupffercell; PAMP, pathogen-associatedmolecular pattern; PMA, phorbolmyristate acetate; SBP, spontaneousbacterial peritonitis; SEC, sinusoidalendothelial cells

* Corresponding author at: Department of Medicine II, University Hospital, LMU Munich, Marchioninistrasse 15, 81377, Munich, Germany.
E-mail address: christian.steib@med.uni-muenchen.de (C.J. Steib).

https://doi.org/10.1016/j.biopha.2020.110208
Received 8 March 2020; Received in revised form 26 April 2020; Accepted 28 April 2020

serum zinc levels [7,8]. *Escherichia coli (E. coli)*, *Enterobacter cloacae (E. cloacae)*, *Enterococcus faecium (E. faecium)* and *Streptococcus pneumoniae (S. pneumoniae)* are the most common pathogens causing SBP. Some strains of these species (such as *E.coli-CFT073*) can induce rapid death of macrophages [5,9,10].

Zinc supplement has been shown to repair pathological changes in animal models with alcoholic injury or infections [11,12]. Many clinical studies have also shown that zinc supplementation had a beneficial effect in severe diarrhea and respiratory infections, especially in infants and children [13]. The effect of zinc supplementation on the infectious diseases is often associated with the number or function of macrophages. Therefore, macrophages is an important cellular target for the anti-infective function of zinc [13]. Highly expressed zinc-dependent endopeptidases in hepatic stellate cells (HSCs) and KCs may also be involved in the progression of fibrosis [8].

Although zinc-related treatments have been reported as new antibacterial weapons, there is still no consensus on dosage, timing and the mechanisms responsible for such effects [14]. In this study, human primary liver non-parenchymal cells [including KCs, HSCs and sinusoidal endothelial cells (SECs)] were treated with bacterial lysates extracted from strains isolated from SBP patients. Combining the clinical data we collected from 2016 to 2019, we aimed to investigate the mechanism of zinc in preventing microbial infections and its clinical application in patients with CLD.

2. Materials and methods

2.1. Study cohort

Totally 149 patients were included, 78 were female and 71 were male. The patient's diagnosis includes: autoimmune hepatitis (AIH, n = 24), chronic viral hepatitis B (HBV, n = 29), chronic viral hepatitis C (HCV, n = 18), primary biliary cholangitis (PBC, n = 6), primary sclerosing cholangitis (PSC, n = 8), alcoholic liver disease (ALD, n = 3), cystic liver disease (n = 2), Budd–Chiari Syndrome (n = 3), M. Wilson disease (n = 1), sarcoidosis (n = 1), liver cirrhosis (including 32 hepatitis-induced, 3 alcohol-induced and 1 Alagille syndrome-induced), nonalcoholic steatohepatitis (NASH, n = 4), cryptogenic cirrhosis (n = 3), toxic liver disease (n = 2), hemochromatosis (n = 2), steatosis hepatitis (n = 5) and liver adenoma (n = 2). The overall zinc concentration was 67.32 ± 21.70 μg/dl and age was 53.34 ± 14.79. The study was approved by the local ethical committee. The laboratory parameters including serum zinc, C-reactive protein (CRP), Leukocytes, Albumin, total bilirubin, Aspartate aminotransferase (GOT), Alanine aminotransferase (GPT), international normalized ratio (INR) and Creatinine were measured by the department of laboratory of the University of hospital of LMU. The above indicators were tested using an automatic analyzer (cobas*8000 modular analyzer series, Roche, Switzerland) and standardized operating procedures according to the manual. Model For End-Stage Liver Disease (MELD) score was calculated as the following formula: MELD Score = 10 * (0.957 * ln (Creatinine) + 0.378 * ln (Bilirubin) + 1.12 * ln (INR) + 0.643).

2.2. Human tissue studies

Human liver tissues were provided by the Biobank of the Department of General, Visceral and Transplantation Surgery, Ludwig-Maximilians University (LMU), Munich, Germany under the administration of the Human Tissue and Cell Research (HTCR) Foundation. The framework of HTCR Foundation [15], which includes obtaining written informed consent from all donors, has been approved by the ethics commission of the Faculty of Medicine at the LMU (approval number 025-12) as well as the Bavarian State Medical Association (approval number 11142), Germany. All experiments were approved by the local government (Regierung von Oberbayern, Munich, Germany) and were reported to the responsible authorities annually. A total of 11 liver tissues were involved in our experiments. Diagnosis of patients included liver metastasis from digestive tract tumor (n = 6), hepatocellular carcinoma (n = 1), liver focal nodular hyperplasia (n = 2), severe liver necrosis (n = 1) and high-risk cholangitis (n = 1).

2.3. Isolation of human primary primary liver non-parenchymal cells

Gradient density centrifugation using Nycodenz gradients (Axis Shield, Rodelokka, Norway) was used to isolate primary liver non-parenchymal cells. Liver tissues were cut into 5–10 mm thick slices and digested for 20 min at 37 °C with pronase (Sigma, St. Louis, USA) and DNase (Roche, Mannheim, Germany). After filtration and centrifugation with fresh Nycodenz solutions (16.7 % for KCs and 28.7 % for HSCs), the mixtures were centrifuged without brake and the interfaces were then collected. Cells were collected and cultured at 37 °C in 5 % CO_2 in RPMI 1640 with fetal calf serum (FCS). To isolate SECs, CD146 MicroBeads (Miltenyi Biotec, Teterow, Germany) and magnetically activated cell sorting system were additionally used. Cells were seeded in plates and cultured at 37 °C in 5 % CO_2. Before stimulation, the medium was changed to RPMI 1640 without FCS for 24 h. Detailed procedures were described in previously published articles [16–18]. Immunofluorescence staining with specific antibodies to liver non-parenchymal cells further confirmed the extracted cells (Fig. 1).

2.4. Cell culture line and treatment

The THP-1 monocytic cell line (American Type Culture Collection, reference number TIB-202™) was a kind gift from Prof. Peter Nelson. Cells were cultured at 37 °C in 5 % CO_2 in RPMI 1640 medium supplemented with 10 % FCS, L-glutamine and streptomycin/penicillin. THP-1 cells differentiated into macrophages by stimulation with 20 ng/mL phorbol myristate (PMA, Sigma, USA) for 24 h [19,20]. Before stimulation, the medium of differentiated THP-1 macrophages (TMCs) was changed to RPMI 1640 without FCS for 24 h.

2.5. Cell stimulation plan

Bacterial strains isolated from patients with SBP including *E. coli, E. cloacae, E. faecium and S. pneumoniae* were involved in this experiment (different group of patients from the study cohort). The isolates were cultured on Columbia 5 % sheep blood media (Becton Dickinson, Heidelberg, Germany) at 37 °C under aeration. The isolates were taken into phosphate buffered solution and washed three times to remove any residual media after growth. Subsequently, the solutions were vortex mixed and checked for sterility after centrifugation and heat inactivation. Extracts were finally diluted to standardized protein concentrations [21]. The isolates were then used to stimulate the relevant cells in certain groups, and the solution of zinc sulfate (ZnSO4, Sigma, USA) was added as well to the stimulation. The supernatants of cells were collected, and immediately frozen and stored at −80 °C before measurement.

2.6. Lactate dehydrogenase (LDH) measurement

The efflux of LDH was measured as an indicator of cell damage, and 5 % Triton-X-100 was used as the 100 % positive control. LDH activity was proportional to the reduction of NAD to NADH. Under NAD catalysis, lactic acid was converted to pyruvate by LDH. The amount of LDH was quantified by the absorbance value at 365 nm according to the rate of NADH production [16,22,23].

2.7. Quantitative reverse transcription PCR (RT-qPCR)

RT-qPCR experiments were performed with the standard protocols. RNA was extracted from human primary KCs and reverse transcribed (total RNA was 1 μg) using the TriFast™ and GoScript™ reverse

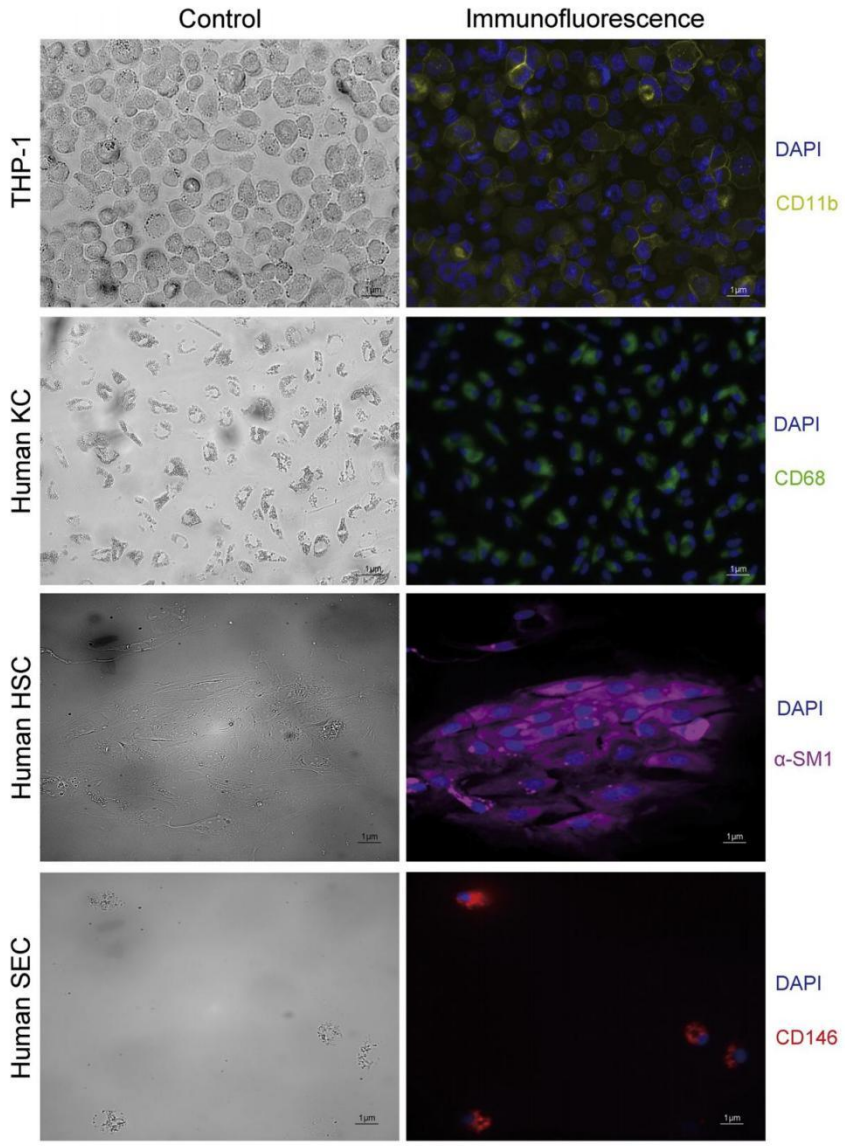

Fig. 1. Immunofluorescence staining results of THP-1 macrophages and human primary non-parenchymal cells.
Anti-CD11b, CD68, α-SM1 and CD146 antibodies were used to confirm the differentiated THP-1 macrophages and primary non-parenchymal cells (including KCs, HSCs and SECs) isolated from human tissues. Each picture was representative from five separate immunostaining results (200x magnification).

transcription system (Promega, USA). The mRNA expression was analyzed by the GoTaq® qPCR Master Mix system (Promega, USA) with specific primers (Table 1). The ABI Prism 7300 sequence detector system (Applied Biosystems, USA) was used for SYBR green qPCR analysis. Relative expression levels of each gene were calculated using the $2^{-\triangle\triangle\alpha}$ method comparing with glyceraldehyde-3-phosphate

Table 1
Primers involved in RT-PCR experiments.

Name	Sequence (5 'to 3')	Fragment
GAPDH	GGAGCGAGATCCCTCCAAAAT GGCTGTTGTCATACTTCTCATGG	197
Myd88	GCATATGCCTGAGCGTTTCG TAGACCAGACACAGGTGCCA	155
MAPK	CTGTTGGACGTTTTTACACCTGC AGACCTGGGAGAATTTGGTAGA	158
NF-κB	GAAGCACGAATGACAGAGGC GCTTGGGGGATTAGCTCTTTT	137
IRAK1	TGAGGAACACGGTGTATGCTG GTTTGGGTGACGAAACCTGGA	119

dehydrogenase (GAPDH).

2.8. ELISA measurement

TXA_2 secretion was quantified from the supernatants of the stimulated cells. TXB_2, the stable degradation product of TXA_2, was measured by TXB_2 ELISA kit (Cayman Chemical, Ann Arbor, MI, USA). The procedures are described in more detail in our previous publications [16,24].

2.9. Confocal microscopy

Primary antibodies against CD11b (1:100; Santa Cruz, Dallas, Texas, USA), CD68 (1:100; Dako, Santa Clara, CA, USA), α-SM1 (1:100; Santa Cruz, Dallas, Texas, USA) and CD146 (1:100; Abcam, London, UK) were used for immunofluorescence. The cells were fixed with 4 % paraformaldehyde (Roth, Karlsruhe, Germany) followed by incubation in blocking buffer (1 % bovine serum albumin, 0.05 % Tween 20 in PBS) for 30 min. After staining with primary antibodies overnight at 4 °C, fluorescent labeled secondary antibodies (Life Technology, Darmstadt, Germany) were added. The cells were analyzed by confocal microscopy (Zeiss LSM 510 META, Jena, Germany).

2.10. Statistical analyses

All data were presented as the mean ± standard deviation (SD) or median and interquartile range (IQR). Normality of data distribution was tested by Kolmogorov-Smirnov Z test (Table 2). The Two-sided Students *t*-test was used for paired or unpaired observations. One-way analysis of variance (ANOVA) or Kruskal Wallis test were used in the comparison of multiple groups. The spearman's rank correlation coefficient was used to measure the potential correlation between zinc and other paraments. A value of $p < 0.05$ was considered to be statistically significant; n denoted the number of samples used. SPSS and Graphpad prism were used for data analysis and figure generation.

Table 2
Normality test of laboratory parameters.

Characteristics	Mean ± SD (N)	K-S test	P value
Age (year)	53.34 ± 14.79 (149)	0.599	0.865
Zinc (mmol/L)	67.32 ± 21.70 (149)	0.727	0.665
Leukocytes (G/L)	6.48 ± 2.39 (147)	1.229	0.097
Albumin (g/dl)	3.86 ± 0.73 (138)	1.894	0.002
CRP (mg/dl)	1.11 ± 2.02 (116)	3.326	< 0.001
Total bilirubin (mg/dl)	2.62 ± 4.62 (149)	3.758	< 0.001
GOT (U/L)	111.65 ± 411.92 (142)	4.875	< 0.001
GPT (U/L)	146.21 ± 649.12 (149)	5.255	< 0.001
INR	1.20 ± 0.40 (149)	2.638	< 0.001
Creatinine (mg/dl)	1.08 ± 0.84 (149)	3.726	< 0.001
Meld score	11.25 ± 6.73 (149)	2.897	< 0.001

K-S test: Kolmogorov-Smirnov Z test. Data are expressed as mean ± SD.

3. Results

3.1. Serum zinc was associated with infection and fibrosis levels in patients with CLD

A total of 149 CLD patients was divided into 3 groups according to the serum zinc levels: low-zinc group (< 60 μg/dl), medium-zinc group (60 − 74 μg/dl) and high-zinc group (≥ 75 μg/dl). Compared with the other two groups, the low-zinc group had lower serum zinc, albumin and GOT levels, while the CRP, total bilirubin, INR, creatinine and MELD scores were significantly higher. In addition, the age in the low-zinc group were also significantly higher than those in the high-zinc group. There were no significant differences between the high-zinc and medium-zinc groups except for serum zinc and CRP levels (Table 3).

According to the results above, using 60 μg/dl as an indicator of zinc deficiency showed better clinical significance. We then divided all patients in only two groups: low-zinc (< 60 mmol/L) and normal-zinc (≥60 mmol/L). Correlations between zinc and other tested indicators were calculated in both groups. The data demonstrated a significant negative correlation between serum zinc levels and CRP and a significant positive correlation between serum zinc and albumin in both groups. Besides, significantly negative correlations were also observed between serum zinc level and total bilirubin, INR or MELD score in the low-zinc group (Table 4).

3.2. Zinc pretreatment protected the injury of bacterial stimulation in TMCs

Dose-response experiments of microbial isolates extracted from SBP patients showed 8 μg/mL was a suitable dosage to cause significant damage in TMCs (Fig. 2A–D). 10–50 μM zinc solution are most commonly used to treat cells and higher concentration is reported to cause direct injury. In our experiments, 24 h treatment with 10 or 20 μM $ZnSO_4$ solution were safe for TMCs, while 50 μM induced significant injury (Fig. 2E). 10 or 20 μM $ZnSO_4$ solution were then added in TMCs for 24 h before bacterial stimulation (zinc 10 or 20 μM pretreatment), only 20 μM could protect against the injury caused by bacterial isolates (Fig. 2F).

3.3. Effects of zinc treatment in bacterial-induced injury in liver non-parenchymal cells

The protective effect of zinc pretreatment (treatment with 20 μM ZnSO4 solution for 24 h prior to bacterial stimulation) was then tested in human liver non-parenchymal cells. Bacterial isolates induced significant LDH increase in KCs, and zinc pretreatment attenuated the increase, however zinc post-treatment (treatment with 20 μM ZnSO4 solution and bacterial isolate simultaneously) did not protect against the injury (Fig. 3A). Bacterial stimulation also caused higher LDH levels in HSCs, but zinc pretreatment was ineffective for this injury (Fig. 3B). No significant changes in LDH levels were found in SECs after bacterial stimulation (Fig. 3C).

3.4. Myd88 related pathway was essential for the protective effect of zinc pretreatment in bacterial-induced injury in KCs

Comparing the effects of zinc pretreatment in hepatic non-parenchymal cells, KC seemed to be the primary target cell for the protective role of zinc in bacterial-induced damage. The possible related pathway for zinc protection was subsequently investigated by RT-qPCR. After bacterial stimulation, the gene expression of myeloid differentiation factor 88 (Myd88), mitogen-associated protein kinase (MAPK) and nuclear factor-kappa B (NF-κB) was significantly increased, while zinc pretreatment reduced the increase (Fig. 4A–C). However, gene expression of interleukin receptor-associated kinase-1 (IRAK-1) did not differ before and after bacterial stimulation (Fig. 4D). TXA_2 is an important effector secreted by KCs after activation, and its role is closely

Table 3
Laboratory parameters based on serum zinc Levels.

Characteristic	High (N)	Medium (N)	Low (N)	P value
Age (year)	48.81 ± 13.93 (58)	54.16 ± 16.15 (38)	57.70 ± 13.50* (53)	0.0055[a]
Sex (Male/Female)	29/29	16/22	26/27	/
Zinc (mmol/L)	88.62 ± 11.26 (58)	67.95 ± 3.86* (38)	43.57 ± 10.44*# (53)	< 0.0001[a]
Leukocytes (G/L)	6.46 ± 1.59 (58)	6.49 ± 2.82 (36)	6.50 ± 2.82 (53)	0.9955[a]
Albumin (g/dl)	4.40(IQR, 4.30 − 4.60) (54)	4.20(IQR, 3.85 − 4.50) (37)	3.50(IQR, 3.00 − 4.00)*# (47)	< 0.0001[b]
CRP (mg/dl)	0.10(IQR, 0.10 − 0.20) (38)	0.30(IQR, 0.10 − 0.55)* (29)	1.30(IQR, 0.55 − 2.60)*# (49)	< 0.0001[b]
Total bilirubin (mg/dl)	0.70(IQR, 0.50 − 1.10) (58)	0.85(IQR, 0.60 − 1.93) (38)	2.70(IQR, 0.95 − 11.2)*# (53)	< 0.0001[b]
GOT (U/L)	28.5(IQR, 25.0 − 37.5) (58)	32.5(IQR, 25.0 − 48.3) (36)	46.0(IQR, 35.3 − 104.0)*# (48)	< 0.0001[b]
GPT (U/L)	30.5(IQR, 22.8 − 49.3) (58)	31.0(IQR, 18.8 − 74.3) (38)	29.0(IQR, 18.5 − 53.5) (53)	0.8326[b]
INR	1.00(IQR, 0.90 − 1.10) (58)	1.00(IQR, 1.00 − 1.30) (38)	1.30(IQR, 1.10 − 1.50)*# (53)	< 0.0001[b]
Creatinine (mg/dl)	0.90(IQR, 0.80 − 1.00) (58)	0.90(IQR, 0.80 − 1.03) (38)	1.10(IQR, 0.90 − 1.30)*# (53)	0.0006[b]
MELD score	6.50(IQR, 6.00 − 8.00) (58)	8.00(IQR, 6.00 − 12.0) (38)	14.0(IQR, 9.50 − 19.0)*# (53)	< 0.0001[b]

Data are expressed as mean ± SD or median and interquartile range (IQR), *p < 0.05, comparing with high group, #p < 0.05, comparing with middle group.
[a] One-way ANOVA analyze.
[b] Kruskal Wallis test.

Table 4
Correlation between zinc level and the other laboratory parameters.

Variables	Zinc (< 60 mmol/L)		Zinc (≥60 mmol/L)		Zinc (all samples)	
	R	P Value	R	P Value	R	P Value
Age	0.089	0.525	−0.196	0.056	−0.273	0.001
CRP	−0.338	0.017	−0.376	0.002	−0.689	< 0.001
Albumin	0.468	0.001	0.397	< 0.001	0.708	< 0.001
Total bilirubin	−0.437	0.001	−0.171	0.097	0.501	< 0.001
GOT	−0.137	0.355	−0.153	0.142	−0.388	< 0.001
INR	−0.490	< 0.001	−0.180	0.080	−0.547	< 0.001
Creatinine	−0.205	0.14	−0.190	0.266	−0.253	0.002
MELD score	−0.503	< 0.001	−0.190	0.064	−0.571	< 0.001

R: Spearman correlation.

related to the Myd88-MAPK related pathway. To confirm the activation of KCs and the MAPK-related pathway during bacterial stimulation, TXB_2 was measured in the supernatants of KCs: all tested bacterial isolates increased TXB_2 in KCs and zinc pretreatment reduced this secretion (Fig. 4E).

4. Discussion

This study investigated the association between serum zinc and other indicators in patients with CLD and the protective mechanisms of zinc in SBP infections. Novel findings in our research were: (1) Low serum zinc levels correlated with higher MELD scores and CRP levels in CLD patients, 60 μg/dl was identified as a threshold for zinc deficiency; (2) Bacterial products induced significant LDH increase in KCs and HSCs, however zinc pretreatment only protected KCs rather than HSCs. (3) Zinc pretreatment, rather than posttreatment, showed protective effects in KCs, and the protection is mediated through the Myd88-MAPK-related pathway. (4) Zinc pretreatment reduced the secretion of TXB_2 in KCs caused by bacterial stimulation.

4.1. Clinical significance of the serum zinc

Systemic inflammation and severe liver fibrosis could induce a decrease in serum zinc concentration. However, due to the lack of specific symptoms, zinc deficiency is always ignored in the clinic. There are various thresholds for zinc deficiency in published articles, the most common being 60 or 75 μg/dl [25–27]. To determine which value is more appropriate, we collected the data from 149 patients with CLD and divided them into three groups based on their serum zinc levels. Serum zinc, albumin, CRP, total bilirubin, GOT, INR, Creatinine and MELD scores in the low-zinc group were significantly different from the other two groups. However, no large differences were found between

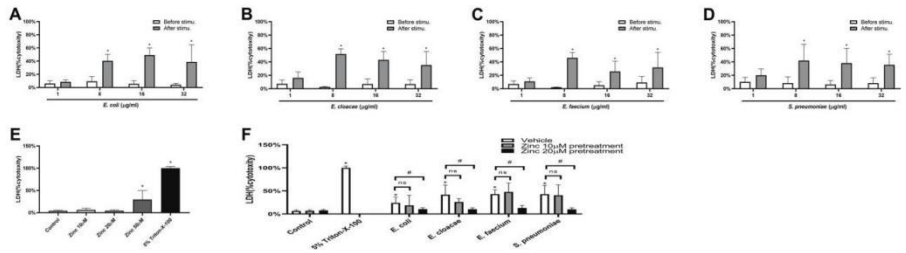

Fig. 2. Effects of zinc pretreatment in THP-1 macrophages following bacterial stimulation.
A–D: Different concentrations of bacterial isolates were used to stimulate differentiated THP-1 macrophages (TMCs), and 8 μg/mL appeared to be a suitable dose for all bacteria (* $p < 0.05$, compared before and after stimulation). E: Treatment of TMCs with 10 or 20 μM ZnSO4 solution (Zinc 10 or 20 μM) for 24 h did not increase LDH levels, whereas 24 h stimulation with 50 μM ZnSO4 solution (Zinc 50 μM) caused direct cell damage (* $p < 0.05$, compared with control group). F: Pretreatment with 20 μM ZnSO4 solution for 24 h in TMCs significantly reduced LDH levels induced by bacterial stimulation, while 10 μM ZnSO4 solution pretreatment showed no protective effect (* $p < 0.05$ compared with vehicle treatment in control group; # $p < 0.05$ compared between vehicle and zinc pretreatment). 5 % Triton-X-100 was used as the positive control. Data were expressed as mean ± SD, ns: no significance, $n = 6$ in each group from three independent experiments.

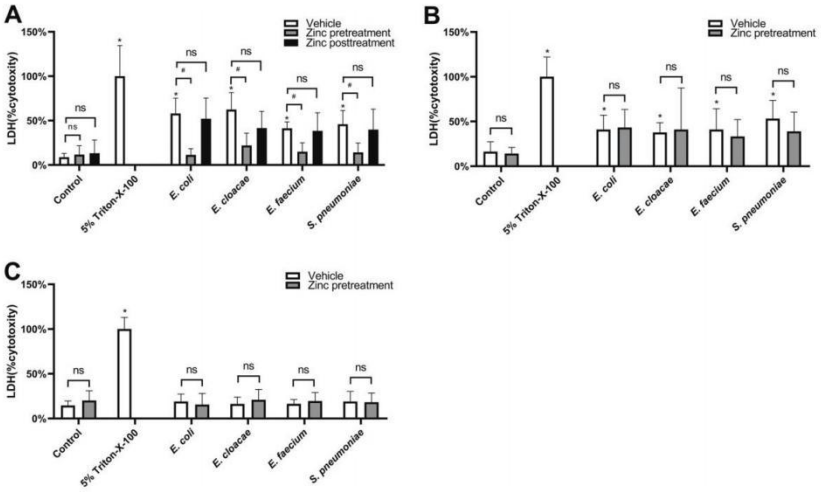

Fig. 3. Effects of zinc treatment on bacterial-induced injury in human liver non-parenchymal cells.
A: Bacterial stimulation (8 μg/mL, 24 h) increased LDH levels in human KCs. Zinc pretreatment (treatment with 20 μM ZnSO4 solution for 24 h before bacterial stimulation) attenuated the LDH increase in KCs, however, Zinc posttreatment (simultaneous treatment with 20 μM ZnSO4 solution and bacterial isolates for 24 h) had no protective effect. B: Bacterial stimulation (8 μg/mL, 24 h) increased LDH levels in human HSCs, but zinc pretreatment failed to reduce the injury. C: Stimulation of human SECs with bacterial isolates (8 μg/mL, 24 h) had no significant effect on LDH concentrations. 5 % Triton-X-100 was used as the positive control. Data were expressed as mean ± SD, $^{*}p < 0.05$ compared with vehicle treatment in control group, $^{\#}p < 0.05$ compared between vehicle and zinc treatment, ns: no significance, n = 6 in each group from three independent experiments with a total of three different human tissues.

the medium-zinc and high-zinc groups. Therefore, using 60 μg/dl as the threshold for zinc deficiency might better distinguish the degree of infection and fibrosis in CLD patients and help to choose the right time to supplement zinc.

We then investigated the correlations between zinc level and the other laboratory parameters in low-zinc (< 60 mmol/L) and normal-zinc (≥60 mmol/L) groups. There was a significant correlation between serum zinc and CRP or albumin in low-zinc, normal-zinc and all populations. Serum albumin is the major zinc-binding protein in the blood and decreases with acute inflammation, while CRP is an acute phase protein that increases with infection [28]. Therefore, serum zinc level was closely related to infections in CLD patients. Different from

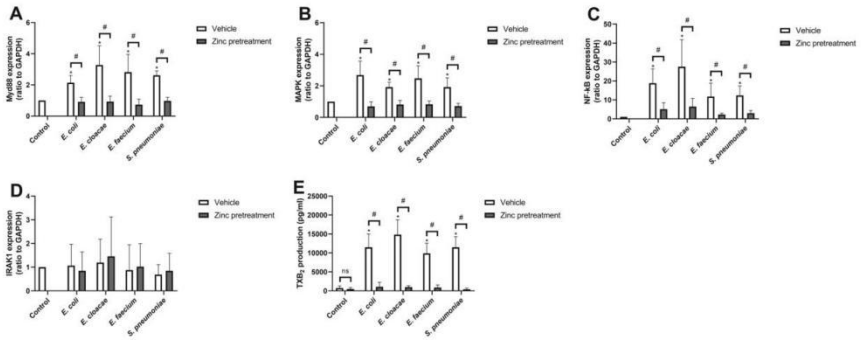

Fig. 4. The Myd88-MAPK related pathway and thromboxane A_2 were involved in the protective effect of zinc pretreatment.
A–D: After stimulation with bacterial isolates (8 μg/mL, 24 h), gene expression of Myd88, MAPK and NF-κB was significantly ($^{*}p < 0.05$ compared with vehicle treatment in control group) increased in human KCs. Pretreatment with 20 μM ZnSO4 solution for 24 h before stimulation (zinc pretreatment) significantly ($^{\#}p < 0.05$ compared between vehicle and zinc treatment) attenuated the increase. The expression of IRAK-1 was not affected by bacterial stimulation. Data were expressed as mean ± SD, n = 5 of five in each group from five independent experiments with a total of five different human tissues. E: Bacterial stimulation significantly ($^{*}p < 0.05$ compared with vehicle treatment in control group) increased the TXB_2 secretion in KCs, which could be reduced ($^{\#}p < 0.05$ compared between vehicle and zinc treatment) by zinc pretreatment. Data were expressed as mean ± SD, n = 6 in each group from three independent experiments with a total of three different human tissues.

the inflammation-related indicators (CRP and albumin), the significant negative correlations between fibrosis-related indicators (total bilirubin, INR and MELD score) and serum zinc occurred only in the low-zinc group. Zinc supplementation can improve the clinical outcome of patients with hepatitis C, regardless of whether they were accompanied with cirrhosis [29,30]. However, there was no significant correlation between changes in serum zinc and changes in MELD scores in patients receiving zinc supplementation [7]. These results indicate that serum zinc in patients with CLD was more related to infection than to fibrosis.

Indeed, zinc supplementation is still an ongoing debate and has to be ruled out in prospective randomized studies. Our human data supported again the necessity to investigate zinc deficiency and zinc supplementation and supported the need to accompany the *in vitro* study to better understand the pathomechanisms of zinc supplementation and zinc deficiency in Kupfer cells. In addition, our human data in part answer the question which boundary value might be preferred in patients with liver diseases.

4.2. The effects of bacterial isolates and zinc supplementation in liver non-parenchymal cells

To investigate the protective mechanism of zinc in bacterial infections, extracts from the four most common pathogens isolated from SBP patients (*E. coli, E. cloacae, E. faecium* and *S. pneumoniae*) were used to stimulate human KCs, HSCs and SECs. SECs account for the highest proportion of non-parenchymal cells in liver, however, the levels of costimulatory molecules (such as CD40, CD80 and CD86) in the SEC are much lower than in HSCs or KCs [31]. Costimulatory molecules are involved in antigen presentation and immune response, which may explain why microbial isolates did not cause an increase in LDH levels in SECs (Fig. 3). Our results were also consistent with previous studies showing that anaphylatoxin C5a can rapidly increase the release of thromboxane A_2 and prostaglandins in KCs and HSCs, but is not in SECs [32].

Recent evidence suggests that regulation of zinc transport in macrophages may play an active role in antibacterial responses. However, the concentration of zinc plays a crucial role: activation of specific pro-inflammatory signaling pathways requires low concentrations of zinc, but high concentrations can inhibit the same pathway [33,34]. Zinc can be phagocytosed and accumulated in KCs. Increased zinc levels in KCs after zinc pretreatment can inhibit inflammatory signaling pathways, thereby reducing damage caused by bacterial stimulation. There is no clear evidence that zinc has an accumulating effect in HSCs, which may be the reason why zinc pretreatment did not reduce the injury to HSCs.

Excessive concentrations of zinc may directly cause cell damage, and in our experiments, 50 μM zinc caused direct injury (Fig. 2E). LPS can trigger rapid accumulation of free zinc in human and mouse macrophages within minutes and reduce serum zinc levels in healthy human volunteers [35,36]. Zinc posttreatment (co-treatment of zinc and bacterial isolates) may cause zinc to accumulate rapidly to excessive concentrations in KCs, resulting in KCs' damage and loss of protection (Fig. 3A).

4.3. Possible mechanisms of the protective effects of zinc in KCs

In addition to choosing the right concentration and conditions, understanding possible antibacterial mechanisms of zinc in KCs is essential to improve the therapeutic results [13]. Most studies related to zinc signaling in macrophages focused on TLR signaling and zinc may act as a key component of many primary TLR signaling events [13]. The Myd88 related pathway is the commonest pathway during TLR activation in macrophages [37–39]. In our experiments, zinc pretreatment attenuated the increased gene expression of Myd88, MAPK and NF-κB caused by bacterial isolates in KCs, suggesting that this pathway plays an important role in the protective effect of zinc.

TXA_2 is mainly secreted by KCs *via* the Myd88-MAPK-related pathway and has recently been identified as an important factor in bacterial defense [40]. In our previous publications, we have demonstrated the important role of TXA_2 in increasing portal perfusion pressure after TLR activation [16,24,41]. The protective effect of zinc pretreatment in KCs and the antibacterial effect of TXA_2 suggested a possible link between zinc and TXA_2 secretion. We then measured the secretion of TXB_2 in KCs after bacterial stimulation: zinc pretreatment significantly reduced TXB_2 secretion caused by all tested bacterial isolates (Fig. 4E). This not only demonstrated the direct effect of zinc on TXA_2 secretion but also verified the association of MAPK-related pathways with zinc. The inhibitory effect of zinc on TXB_2 secretion may also explain the association between zinc deficiency and prehypertension in previous studies [42].

5. Conclusion

Serum zinc levels may be a valuable marker for assessing the severity of infection and liver fibrosis in patients with CLD. In addition, our results deepen our understanding of zinc supplementation as an antimicrobial weapon: Zinc pretreatment reduces inflammation and TXA_2 secretion by inhibiting the activation of the Myd88-MAPK-NF-κB pathway in KCs.

Funding sources

This study was supported by the Deutsche Forschungsgemeinschaft under Grant Number DFG STE 1022/2-3 and DFG STE 1022/4-1; China Scholarship Council under grant Number 201606230249 and 201908080017; and the Human Tissue and Cell Research Foundation, a non-profit foundation regulated by German civil law.

Declaration of Competing Interest

The authors declare no conflicts of interest.

Acknowledgements

The authors thank Ingrid Liss and Christoph v. Hesler for their excellent technical assistance.

References

[1] P.Z. Sobocinski, W.J. Canterbury Jr., C.A. Mapes, et al., Involvement of hepatic metallothioneins in hypozincemia associated with bacterial infection, Am. J. Physiol. 234 (4) (1978) E399–406, https://doi.org/10.1152/ajpendo.1978.234.4.E399.
[2] C. Acharya, N. Dharel, R.K. Sterling, Chronic liver disease in the human immunodeficiency virus patient, Clin. Liver Dis. 19 (1) (2015) 1–22, https://doi.org/10.1016/j.cld.2014.09.001.
[3] J. King, S.F. Brunel, A. Warris, Aspergillus infections in cystic fibrosis, J. Infect. (Suppl. 72) (2016) S50–55, https://doi.org/10.1016/j.jinf.2016.04.022.
[4] J.S. Bajaj, Review article: potential mechanisms of action of rifaximin in the management of hepatic encephalopathy and other complications of cirrhosis, Aliment. Pharmacol. Ther. 43 (Suppl. 1) (2016) 11–26, https://doi.org/10.1111/apt.13435.
[5] C.J. Steib, J. Schewe, A.L. Gerbes, Infection as a trigger for portal hypertension, Dig. Dis. 33 (4) (2015) 570–576, https://doi.org/10.1159/000375352.
[6] A.A. Nanji, E.C. Liong, J. Xiao, et al., Thromboxane inhibitors attenuate inflammatory and fibrotic changes in rat liver despite continued ethanol administrations, Alcohol. Clin. Exp. Res. 37 (1) (2013) 31–39, https://doi.org/10.1111/j.1530-0277.2012.01838.x.
[7] S. Sengupta, K. Wroblewski, A. Aronsohn, et al., Screening for zinc deficiency in patients with cirrhosis: when should we start? Dig. Dis. Sci. 60 (10) (2015) 3130–3135, https://doi.org/10.1007/s10620-015-3613-0.
[8] K. Friedrich, C. Baumann, M. Brune, et al., Association of serum zinc levels with liver function and survival in patients awaiting liver transplantation, Langenbecks Arch. Surg. 400 (7) (2015) 805–811, https://doi.org/10.1007/s00423-015-1334-7.
[9] V. Arvaniti, G. D'Amico, G. Fede, et al., Infections in patients with cirrhosis increase mortality four-fold and should be used in determining prognosis, Gastroenterology 139 (4) (2010), https://doi.org/10.1053/j.gastro.2010.06.019 1246-56, 56 e1-5.
[10] C.J. Stocks, M.D. Phan, M.E.S. Achard, et al., Uropathogenic Escherichia coli employs both evasion and resistance to subvert innate immune-mediated zinc toxicity for dissemination, Proc. Natl. Acad. Sci. U. S. A. 116 (13) (2019) 6341–6350,

https://doi.org/10.1073/pnas.1820870116.
[11] S. Bao, M.J. Liu, B. Lee, et al., Zinc modulates the innate immune response in vivo to polymicrobial sepsis through regulation of NF-kappaB, Am. J. Physiol. Lung Cell Mol. Physiol. 298 (6) (2010) L744–54, https://doi.org/10.1152/ajplung.00368.2009.
[12] Y.H. Cho, S.J. Lee, S.J.Y. Lee, et al., Antibacterial effect of intraprostatic zinc injection in a rat model of chronic bacterial prostatitis, Int. J. Antimicrob. Agents 19 (6) (2002) 576–582, https://doi.org/10.1016/s0924-8579(02)00115-2.
[13] S.L. Stafford, N.J. Bokil, M.E. Achard, et al., Metal ions in macrophage antimicrobial pathways: emerging roles for zinc and copper, Biosci. Rep. 33 (4) (2013), https://doi.org/10.1042/BSR20130014.
[14] S. Buracco, B. Peracino, C. Andreini, et al., Differential effects of Iron, zinc, and copper on dictyostelium discoideum cell growth and resistance to Legionella pneumophila, Front. Cell. Infect. Microbiol. 7 (2017) 536, https://doi.org/10.3389/fcimb.2017.00536.
[15] W.E. Thasler, T.S. Weiss, K. Schillhorn, et al., Charitable state-controlled foundation human tissue and cell research: ethic and legal aspects in the supply of surgically removed human tissue for research in the academic and commercial sector in Germany, Cell Tissue Bank. 4 (1) (2003) 49–56, https://doi.org/10.1023/A:1026392429112.
[16] C.J. Steib, M. Bilzer, M. op den Winkel, et al., Treatment with the leukotriene inhibitor montelukast for 10 days attenuates portal hypertension in rat liver cirrhosis, Hepatology 51 (6) (2010) 2086–2096, https://doi.org/10.1002/hep.23596.
[17] C.J. Steib, L. Gmelin, S. Pfeiler, et al., Functional relevance of the cannabinoid receptor 2 - heme oxygenase pathway: a novel target for the attenuation of portal hypertension, Life Sci. 93 (16) (2013) 543–551, https://doi.org/10.1016/j.lfs.2013.08.018.
[18] V. Kegel, D. Deharde, E. Pfeiffer, et al., Protocol for isolation of primary human hepatocytes and corresponding major populations of non-parenchymal liver cells, J. Vis. Exp. (109) (2016) e53069, https://doi.org/10.3791/53069.
[19] E. Stachowska, V. Dziedziejko, K. Safranow, et al., Effect of conjugated linoleic acids on the activity and mRNA expression of 5- and 15-lipoxygenases in human macrophages, J. Agric. Food Chem. 55 (13) (2007) 5335–5342, https://doi.org/10.1021/jf0701077.
[20] J.C. Price, J. Cronin, I.M. Sheldon, Toll-like receptor expression and function in the COV434 granulosa cell line, Am. J. Reprod. Immunol. 68 (3) (2012) 205–217, https://doi.org/10.1111/j.1600-0897.2011.01103.x.
[21] A. Wieser, E. Romann, G. Magistro, et al., A multiepitope subunit vaccine conveys protection against extraintestinal pathogenic Escherichia coli in mice, Infect. Immun. 78 (8) (2010) 3432–3442, https://doi.org/10.1128/IAI.00174-10.
[22] C.J. Steib, A.C. Hartmann, C. v Hesler, et al., Intraperitoneal LPS amplifies portal hypertension in rat liver fibrosis, Lab. Invest. 90 (7) (2010) 1024–1032, https://doi.org/10.1038/labinvest.2010.60.
[23] M. op den Winkel, L. Gmelin, J. Schewe, et al., Role of cysteinyl-leukotrienes for portal pressure regulation and liver damage in cholestatic rat livers, Lab. Invest. 93 (12) (2013) 1288–1294, https://doi.org/10.1038/labinvest.2013.115.
[24] C.J. Steib, A.L. Gerbes, M. Bystron, et al., Kupffer cell activation in normal and fibrotic livers increases portal pressure via thromboxane A(2), J. Hepatol. 47 (2) (2007) 228–238, https://doi.org/10.1016/j.jhep.2007.03.019.
[25] H.C. Chao, Y.J. Chang, W.L. Huang, Cut-off serum zinc concentration affecting the appetite, growth, and nutrition status of undernourished children supplemented with zinc, Nutr. Clin. Pract. 33 (5) (2018) 701–710, https://doi.org/10.1002/ncp.10079.
[26] E.B. Fung, G. Gildengorin, S. Talwar, et al., Zinc status affects glucose homeostasis and insulin secretion in patients with thalassemia, Nutrients 7 (6) (2015) 4296–4307, https://doi.org/10.3390/nu7064296.
[27] N. Khalid, A. Ahmed, M.S. Bhatti, et al., A question mark on zinc deficiency in 185 million people in Pakistan–possible way out, Crit. Rev. Food Sci. Nutr. 54 (9) (2014) 1222–1240, https://doi.org/10.1080/10408398.2011.630541.
[28] V. Vatsalya, M. Kong, M.C. Cave, et al., Association of serum zinc with markers of liver injury in very heavy drinking alcohol-dependent patients, J. Nutr. Biochem. 59 (2018) 49–55, https://doi.org/10.1016/j.jnutbio.2018.05.003.
[29] S. Matsuoka, H. Matsumura, H. Nakamura, et al., Zinc supplementation improves the outcome of chronic hepatitis C and liver cirrhosis, J. Clin. Biochem. Nutr. 45 (3) (2009) 292–303, https://doi.org/10.3164/jcbn.08-246.
[30] H. Matsumura, K. Nirei, H. Nakamura, et al., Zinc supplementation therapy improves the outcome of patients with chronic hepatitis C, J. Clin. Biochem. Nutr. 51 (3) (2012) 178–184, https://doi.org/10.3164/jcbn.12-11.
[31] X.K. Xing, H.Y. Wu, H.G. Feng, et al., Immune function of nonparenchymal liver cells, Genet. Mol. Res. 15 (1) (2016), https://doi.org/10.4238/gmr.15018524.
[32] H.L. Schieferdecker, S. Pestel, G.P. Puschel, et al., Increase by anaphylatoxin C5a of glucose output in perfused rat liver via prostanoids derived from nonparenchymal cells: direct action of prostaglandins and indirect action of thromboxane A(2) on hepatocytes, Hepatology 30 (2) (1999) 454–461, https://doi.org/10.1002/hep.510300229.
[33] J.A. Lemire, J.J. Harrison, R.J. Turner, Antimicrobial activity of metals: mechanisms, molecular targets and applications, Nat. Rev. Microbiol. 11 (6) (2013) 371–384, https://doi.org/10.1038/nrmicro3028.
[34] H. Haase, L. Rink, Signal transduction in monocytes: the role of zinc ions, Biometals 20 (3–4) (2007) 579–585, https://doi.org/10.1007/s10534-006-9029-8.
[35] H. Haase, J.L. Ober-Blobaum, G. Engelhardt, et al., Zinc signals are essential for lipopolysaccharide-induced signal transduction in monocytes, J. Immunol. 181 (9) (2008) 6491–6502, https://doi.org/10.4049/jimmunol.181.9.6491.
[36] L.M. Gaetke, C.J. McClain, R.T. Talwalkar, et al., Effects of endotoxin on zinc metabolism in human volunteers, Am. J. Physiol. 272 (6 Pt 1) (1997) E952–6, https://doi.org/10.1152/ajpendo.1997.272.6.E952.
[37] H. Kalvegren, C. Skoglund, C. Helldahl, et al., Toll-like receptor 2 stimulation of platelets is mediated by purinergic P2X1-dependent Ca2+ mobilisation, cyclooxygenase and purinergic P2Y1 and P2Y12 receptor activation, Thromb. Haemost. 103 (2) (2010) 398–407, https://doi.org/10.1160/TH09-07-0442.
[38] B.M. Thobe, M. Frink, F. Hildebrand, et al., The role of MAPK in Kupffer cell toll-like receptor (TLR) 2-, TLR4-, and TLR9-mediated signaling following trauma-hemorrhage, J. Cell. Physiol. 210 (3) (2007) 667–675, https://doi.org/10.1002/jcp.20860.
[39] K. Falker, K. Klarstrom-Engstrom, T. Bengtsson, et al., The toll-like receptor 2/1 (TLR2/1) complex initiates human platelet activation via the src/Syk/LAT/PLCgamma2 signalling cascade, Cell. Signal. 26 (2) (2014) 279–286, https://doi.org/10.1016/j.cellsig.2013.11.011.
[40] Y. Yoshikai, Roles of prostaglandins and leukotrienes in acute inflammation caused by bacterial infection, Curr. Opin. Infect. Dis. 14 (3) (2001) 257–263, https://doi.org/10.1097/00001432-200106000-00003.
[41] J. Zhang, J. Schewe, H. Li, et al., The effects of hepatic steatosis on thromboxane A2 induced portal hypertension, Gastroenterol. Hepatol. 42 (9) (2019) 534–541, https://doi.org/10.1016/j.gastrohep.2019.03.015.
[42] S.C. Nevarez-Lopez, L.E. Simental-Mendia, F. Guerrero-Romero, et al., Zinc deficiency is an independent risk factor for prehypertension in healthy subjects, Int. J. Vitam. Nutr. Res. (2019) 1–6, https://doi.org/10.1024/0300-9831/a000593.

9 References

[1] Siegel RL, Miller KD, Jemal A. Cancer statistics, 2019[J]. CA Cancer J Clin. 2019 Jan;69(1):7-34.
[2] Bruix J, Sherman M. Management of hepatocellular carcinoma: an update[J]. Hepatology. 2011 Mar;53(3):1020-2. Cancer J Clin. 2019 Jan;69(1):7-34.
[3] Llovet JM, Ricci S, Mazzaferro V, et al. Sorafenib in advanced hepatocellular carcinoma[J].N Engl J Med. 2008 Jul 24;359(4):378-90.
[4] Zhang M, He Y, Zhang X, et al. A pooled analysis of the diagnostic efficacy of plasmic methylated septin-9 as a novel biomarker for colorectal cancer[J].Biomed Rep. 2017 Oct;7(4):353-360.
[5] Poüs C, Klipfel L, Baillet A. Cancer-Related Functions and Subcellular Localizations of Septins.[J].Front Cell Dev Biol. 2016 Nov 8;4:126.
[6] Fung K Y, Dai L, Trimble W S. Cell and molecular biology of septins[J]. Int Rev Cell Mol Biol, 2014,310:289-339.
[7] Gebhard C, Miller I, Hummel K, et al. Comparative proteome analysis of monolayer and spheroid culture of canine osteosarcoma cells[J]. J Proteomics, 2018.
[8] Khan A, Newby J, Gladfelter A S. Control of septin filament flexibility and bundling by subunit composition and nucleotide interactions[J]. Mol Biol Cell, 2018.
[9] Schwan C, Aktories K. Formation of Nanotube-Like Protrusions, Regulation of Septin Organization and Re-guidance of Vesicle Traffic by Depolymerization of the Actin Cytoskeleton Induced by Binary Bacterial Protein Toxins[J]. Curr Top Microbiol Immunol, 2017,399:35-51.
[10] Caudron F, Yadav S. Meeting report - shining light on septins[J]. J Cell Sci, 2018,131(1).
[11] Akhmetova K, Balasov M, Svitin A, et al. Phosphorylation of Pnut in the Early Stages of Drosophila Embryo Development Affects Association of the Septin Complex with the Membrane and Is Important for Viability[J]. G3 (Bethesda), 2018,8(1):27-38.
[12] Perez A M, Finnigan G C, Roelants F M, et al. Septin-Associated Protein Kinases in the Yeast Saccharomyces cerevisiae[J]. Front Cell Dev Biol, 2016,4:119.
[13] Angelis D, Spiliotis E T. Septin Mutations in Human Cancers[J]. Front Cell Dev Biol, 2016,4:122.
[14] Glomb O, Gronemeyer T. Septin Organization and Functions in Budding Yeast[J]. Front Cell Dev Biol, 2016,4:123.
[15] Ostevold K, Melendez A V, Lehmann F, et al. Septin remodeling is essential for the formation of cell membrane protrusions (microtentacles) in detached tumor cells[J]. Oncotarget, 2017,8(44):76686-76698.
[16] Valadares N F, D' M P H, Ulian A A, et al. Septin structure and filament assembly[J]. Biophys Rev, 2017,9(5):481-500.
[17] Torraca V, Mostowy S. Septins and Bacterial Infection[J]. Front Cell Dev Biol, 2016,4:127.
[18] Barve G, Sridhar S, Aher A, et al. Septins are involved at the early stages of macroautophagy in S. cerevisiae[J]. J Cell Sci, 2018,131(4).

[19]Song K, Russo G, Krauss M. Septins As Modulators of Endo-Lysosomal Membrane Traffic[J]. Front Cell Dev Biol, 2016,4:124.
[20]Momany M, Talbot N J. Septins Focus Cellular Growth for Host Infection by Pathogenic Fungi[J]. Front Cell Dev Biol, 2017,5:33.
[21]Heasley L R, McMurray M A. Small molecule perturbations of septins[J]. Methods Cell Biol, 2016,136:311-319.
[22]Spiliotis E T. Spatial effects - site-specific regulation of actin and microtubule organization by septin GTPases[J]. J Cell Sci, 2018,131(1).
[23]Yanshina D D, Kossinova O A, Gopanenko A V, et al. Structural features of the interaction of the 3'-untranslated region of mRNA containing exosomal RNA-specific motifs with YB-1, a potential mediator of mRNA sorting[J]. Biochimie, 2018,144:134-143.
[24]Orellana-Munoz S, Duenas-Santero E, Arnaiz-Pita Y, et al. The anillin-related Int1 protein and the Sep7 septin collaborate to maintain cellular ploidy in Candida albicans[J]. Sci Rep, 2018,8(1):2257.
[25]Pagliuso A, Cossart P, Stavru F. The ever-growing complexity of the mitochondrial fission machinery[J]. Cell Mol Life Sci, 2018,75(3):355-374.
[26]Neubauer K, Zieger B. The Mammalian Septin Interactome[J]. Front Cell Dev Biol, 2017,5:3.
[27]Onishi M, Pringle J R. The nonopisthokont septins: How many there are, how little we know about them, and how we might learn more[J]. Methods Cell Biol, 2016,136:1-19.
[28]Cannon K S, Woods B L, Gladfelter A S. The Unsolved Problem of How Cells Sense Micron-Scale Curvature[J]. Trends Biochem Sci, 2017,42(12):961-976.
[29]Palander O, El-Zeiry M, Trimble W S. Uncovering the Roles of Septins in Cilia[J]. Front Cell Dev Biol, 2017,5:36.
[30]Lee P P, Lobato-Marquez D, Pramanik N, et al. Wiskott-Aldrich syndrome protein regulates autophagy and inflammasome activity in innate immune cells[J]. Nat Commun, 2017,8(1):1576.
[31]Borkhardt A, Teigler-Schlegel A, Fuchs U, et al. An ins(X;11)(q24;q23) fuses the MLL and the Septin 6/KIAA0128 gene in an infant with AML-M2[J]. Genes Chromosomes Cancer, 2001,32(1):82-88.
[32]Ihara M, Tomimoto H, Kitayama H, et al. Association of the cytoskeletal GTP-binding protein Sept4/H5 with cytoplasmic inclusions found in Parkinson's disease and other synucleinopathies[J]. J Biol Chem, 2003,278(26):24095-24102.
[33]Shih L Y, Liang D C, Fu J F, et al. Characterization of fusion partner genes in 114 patients with de novo acute myeloid leukemia and MLL rearrangement[J]. Leukemia, 2006,20(2):218-223.
[34]Schwindt H, Vater I, Kreuz M, et al. Chromosomal imbalances and partial uniparental disomies in primary central nervous system lymphoma[J]. Leukemia, 2009,23(10):1875-1884.
[35]Lee S G, Park T S, Oh S H, et al. De novo acute myeloid leukemia associated with t(11;17)(q23;q25) and MLL-SEPT9 rearrangement in an elderly patient: a case study and review of the literature[J]. Acta Haematol, 2011,126(4):195-198.

[36]Ono R, Nakajima H, Ozaki K, et al. Dimerization of MLL fusion proteins and FLT3 activation synergize to induce multiple-lineage leukemogenesis[J]. J Clin Invest, 2005,115(4):919-929.
[37]Ono R, Ihara M, Nakajima H, et al. Disruption of Sept6, a fusion partner gene of MLL, does not affect ontogeny, leukemogenesis induced by MLL-SEPT6, or phenotype induced by the loss of Sept4[J]. Mol Cell Biol, 2005,25(24):10965-10978.
[38]Santos J, Cerveira N, Bizarro S, et al. Expression pattern of the septin gene family in acute myeloid leukemias with and without MLL-SEPT fusion genes[J]. Leuk Res, 2010,34(5):615-621.
[39]Kojima K, Sakai I, Hasegawa A, et al. FLJ10849, a septin family gene, fuses MLL in a novel leukemia cell line CNLBC1 derived from chronic neutrophilic leukemia in transformation with t(4;11)(q21;q23)[J]. Leukemia, 2004,18(5):998-1005.
[40]Cerveira N, Lisboa S, Correia C, et al. Genetic and clinical characterization of 45 acute leukemia patients with MLL gene rearrangements from a single institution[J]. Mol Oncol, 2012,6(5):553-564.
[41]Kim H J, Ki C S, Park Q, et al. MLL/SEPTIN6 chimeric transcript from inv ins(X;11)(q24;q23q13) in acute monocytic leukemia: report of a case and review of the literature[J]. Genes Chromosomes Cancer, 2003,38(1):8-12.
[42]Kadkol S S, Bruno A, Oh S, et al. MLL-SEPT6 fusion transcript with a novel sequence in an infant with acute myeloid leukemia[J]. Cancer Genet Cytogenet, 2006,168(2):162-167.
[43]Cerveira N, Bizarro S, Teixeira M R. MLL-SEPTIN gene fusions in hematological malignancies[J]. Biol Chem, 2011,392(8-9):713-724.
[44]Fu J F, Liang D C, Yang C P, et al. Molecular analysis of t(X;11)(q24;q23) in an infant with AML-M4[J]. Genes Chromosomes Cancer, 2003,38(3):253-259.
[45]Meyer C, Kowarz E, Hofmann J, et al. New insights to the MLL recombinome of acute leukemias[J]. Leukemia, 2009,23(8):1490-1499.
[46]Strehl S, Konig M, Meyer C, et al. Molecular dissection of t(11;17) in acute myeloid leukemia reveals a variety of gene fusions with heterogeneous fusion transcripts and multiple splice variants[J]. Genes Chromosomes Cancer, 2006,45(11):1041-1049.
[47]Ono R, Taki T, Taketani T, et al. SEPTIN6, a human homologue to mouse Septin6, is fused to MLL in infant acute myeloid leukemia with complex chromosomal abnormalities involving 11q23 and Xq24[J]. Cancer Res, 2002,62(2):333-337.
[48]Santos J, Cerveira N, Correia C, et al. Coexistence of alternative MLL-SEPT9 fusion transcripts in an acute myeloid leukemia with t(11;17)(q23;q25)[J]. Cancer Genet Cytogenet, 2010,197(1):60-64.
[49]Xiangji L, Feng X, Qingbao C, et al. Knockdown of HBV surface antigen gene expression by a lentiviral microRNA-based system inhibits HBV replication and HCC growth[J]. J Viral Hepat, 2011,18(9):653-660.
[50]Xiangji L, Feng X, Qingbao C, et al. Knockdown of HBV surface antigen gene expression by a lentiviral microRNA-based system inhibits HBV replication and HCC growth[J]. J Viral Hepat, 2011,18(9):653-660.
[51]Yu W, Ding X, Chen F, et al. The phosphorylation of SEPT2 on Ser218 by casein

kinase 2 is important to hepatoma carcinoma cell proliferation[J]. Mol Cell Biochem, 2009,325(1-2):61-67.

10 Acknowledgements

First of all, I would like to show my deep appreciation to Prof. Dr. med. Christian J. Steib for granting me the valuable opportunity to work in the Department of Medicine II, Liver Center Munich, Klinikum Großhadern as a doctoral student. And I really appreciate the support, advice and trust he provided from the bottom of my heart. I won't have my publication without his supports. His enthusiasm and wisdom for scientific research motivated me a lot and from his excellent scientific knowledge I could also learn a lot in the last years.

My sincere thanks also to Prof. Julia Mayerle who provided me help and advices in my academic life. I would love to signify my special thanks to Hao Lin, Jiang Zhang, Hanwei Li, Christoph von Hesler and Ingrid Liss. Thanks for their kind aid and support every time I needed, for thier guidance and technical assistance, and all the joy that fortified my daily life! I am so appreciated being a member in such a supportive and considerate working group.

My thanks also go to Yonggan Xue, Liangtao Ye who are also doctoral students in the same lab. We studied in the lab during a similar time period and grew together. I'm so grateful that they shared a lot of experimental experience which helped me a lot. I wish you all success in your study and life.

My special thanks to my family for their support, faith and love in me during any time in my life and to my friends for encouraging me and having enjoyable times out of the working.

Thanks to the excellent platform of LMU, not only the precise and advanced equipment, but also the rigorous academic attitude of the professors and teachers, the diligent working atmosphere of my colleagues, all have laid a good foundation for my scientific research and study in Munich. Also special thanks go to China Scholarship Council, who gave me the finical support and alleviated my economic burden a lot.

Finally, thanks to the experience here over the past years, these changes are deeply imprinted in my memory,witnessing my growth. I hope this dissertation will not be the end of my academic thinking, but a start instead.